

AD-A089 972

NAVAL POSTGRADUATE SCHOOL MONTEREY CA

F/0 8/10

PREDICTION OF THE SPRING TRANSITION AND RELATED SEA-SURFACE TEM--ETC(U)

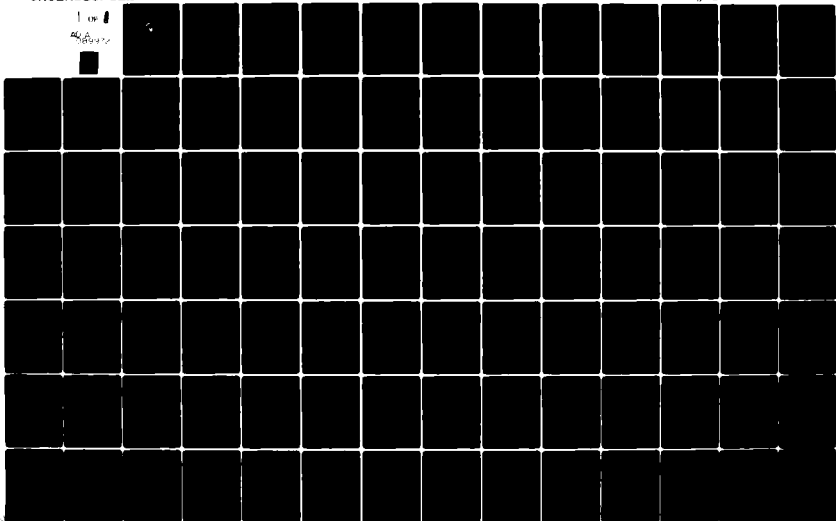
JUN 80 B W BUDD

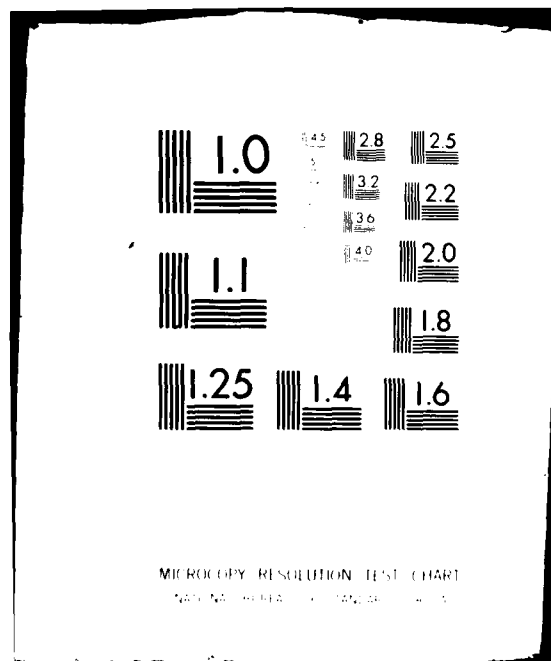
NL

UNCLASSIFIED

1 of 1

AD-A089 972



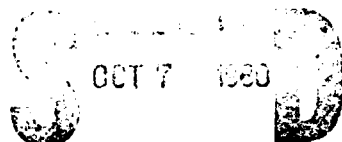


AD A089972

NAVAL POSTGRADUATE SCHOOL  
Monterey, California



THESIS



A

PREDICTION OF THE SPRING TRANSITION  
AND RELATED SEA-SURFACE  
TEMPERATURE ANOMALIES

by

Bruce Warren Budd

June 1980

Thesis Advisor:

R. L. Elsberry

Approved for public release; distribution unlimited

DDC FILE COPY

80 10 3 089

REPORT DOCUMENTATION PAGE		READ INSTRUCTIONS BEFORE COMPLETING FORM	
1. REPORT NUMBER	2. GOVT ACCESSION NO.	3. RECIPIENT'S CATALOG NUMBER	
	AD-A089	973	
4. TITLE (and Subtitle)		5. TYPE OF REPORT & PERIOD COVERED	
Prediction of the Spring Transition and Related Sea-Surface Temperature Anomalies		⑨ Master's Thesis; June 1980	
7. AUTHOR(s)		8. PERFORMING ORG. REPORT NUMBER	
Bruce Warren/Budd			
9. PERFORMING ORGANIZATION NAME AND ADDRESS		10. CONTRACT OR GRANT NUMBER(s)	
Naval Postgraduate School ✓ Monterey, California 93940		(12) 162	
11. CONTROLLING OFFICE NAME AND ADDRESS		12. REPORT DATE	
Naval Postgraduate School Monterey, California		June 1980	
14. MONITORING AGENCY NAME & ADDRESS (if different from Controlling Office)		13. NUMBER OF PAGES	
		95	
		15. SECURITY CLASS. (of this report)	
		Unclassified	
		15a. DECLASSIFICATION/DOWNGRADING SCHEDULE	
16. DISTRIBUTION STATEMENT (of this Report)			
Approved for public release; distribution unlimited.			
17. DISTRIBUTION STATEMENT (of the abstract entered in Block 20, if different from Report)			
18. SUPPLEMENTARY NOTES			
19. KEY WORDS (Continue on reverse side if necessary and identify by block number)			
1-D ocean modeling, SST anomaly, mixed layer dynamics, upper ocean prediction.			
20. ABSTRACT (Continue on reverse side if necessary and identify by block number)			
<p>A hypothesis by Elsberry and Garwood (1978) for generation of upper ocean temperature anomalies during the spring transition period was tested. If the transition between the winter and summer regimes occurred earlier (later) than normal, the seasonal heating was expected to have been accumulated in a shallow (deep) layer, and would have tended to produce a positive (negative) sea-surface temperature anomaly.</p>			

Block #20 cont.

The Garwood (1977) one-dimensional, oceanic mixed layer model was used to predict the thermal structure changes, from March 15 to July 15 during 1976 and 1977. The forcing fields from the atmospheric prediction model of Fleet Numerical Oceanography Center (FNOC) were interpolated to hourly intervals. The suitability of the FNOC heat flux calculations was examined through comparison with the observed upper ocean heat content changes derived from the TRANSPAC data. The recomputed mixed layer depth and temperature responses from the adjusted heat flux fields were used, in lieu of the original calculations, because of the improvement in the behavior of the time series predictions. Weather maps and atmospheric forcing fields were used in describing the meteorological conditions associated with the transition period. The model-predicted spatial and temporal distribution of the spring transition over the NORPAX Anomaly Dynamics Study (ADS) region varied between 1976 and 1977. The relationship between the transition dates and the generation and persistence of thermal structure anomalies during the following months was generally supported by the model predictions.

A

Approved for public release; distribution unlimited

Prediction of the Spring Transition  
And Related Sea-Surface Temperature Anomalies

by

Bruce Warren Budd  
B.S., University of Utah, 1974

Submitted in partial fulfillment of the  
requirements for the degree of

MASTER OF SCIENCE IN METEOROLOGY

from the

NAVAL POSTGRADUATE SCHOOL  
June 1980

Author

Bruce W. Budd

Approved by:

Russell L. Elsberry

Thesis Advisor

Roland W. Garwood Jr.

Co-Advisor

G. J. Haltiner

Chairman, Department of Meteorology

William M. Tolles

Dean of Science and Engineering

## ABSTRACT

↙  
A hypothesis by Elsberry and Garwood (1978) for generation of upper ocean temperature anomalies during the spring transition period was tested. If the transition between the winter and summer regimes occurred earlier (later) than normal, the seasonal heating was expected to have been accumulated in a shallow (deep) layer, and would have tended to produce a positive (negative) sea-surface temperature anomaly.

The Garwood (1977) one-dimensional, oceanic mixed-layer model was used to predict the thermal structure changes, from March 15 to July 15 during 1976 and 1977. The forcing fields from the atmospheric prediction model of Fleet Numerical Oceanography Center (FNOC) were interpolated to hourly intervals. The suitability of the FNOC heat flux calculations was examined through comparison with the observed upper ocean heat content changes derived from the TRANSPAC data. The recomputed mixed-layer depth and temperature responses from the adjusted heat flux fields were used, in lieu of the original calculations, because of the improvement in the behavior of the time series predictions. Weather maps and atmospheric forcing fields were used in describing the meteorological conditions associated with the transition period. The model-predicted spatial and temporal distribution of the spring transition over the NORPAX Anomaly Dynamics

↘ next page

Cont. Study (ADS) region varied between 1976 and 1977. The relationship between the transition dates and the generation and persistence of thermal structure anomalies during the following months was generally supported by the model predictions.



## TABLE OF CONTENTS

LIST OF TABLES .....	8
LIST OF FIGURES .....	9
ACKNOWLEDGEMENTS .....	12
I. INTRODUCTION .....	13
A. HYPOTHESIS .....	13
B. BACKGROUND .....	13
1. Synoptic Time-Scale .....	14
2. Diurnal Time-Scale .....	14
3. Atmospheric Friction Velocity ( $u_*$ ) ----	15
4. Spring Transition .....	16
5. Development of SST Anomalies .....	17
C. STUDY DESCRIPTION .....	19
II. COMPARISON OF HEAT CONTENT WITH CUMULATIVE SURFACE HEAT FLUX .....	22
A. HEAT CONTENT .....	22
B. CUMULATIVE HEAT FLUX .....	26
C. ADJUSTMENTS TO HEAT FLUX .....	27
III. TIME SERIES OF FORCING FUNCTIONS .....	35
A. WIND SPEED .....	35
B. SOLAR RADIATION FLUX .....	38
C. TOTAL HEAT FLUX .....	38
D. EXAMPLES DURING SPRING TRANSITION .....	39
IV. OCEAN THERMAL STRUCTURE - PREDICTION/VERIFICATION	41
A. PREDICTION OF MIXED LAYER DEPTH AND TEMPERATURE .....	41

1. Zonal Section -----	41
2. Meridional Section -----	44
B. TEMPERATURE PROFILES -----	49
V. CHARACTERISTICS OF TWO NORTHERN LOCATIONS -----	53
VI. ADJUSTED HEAT FLUX AT 30°N, 175°W IN 1977 -----	60
VII. SPRING TRANSITION -----	64
A. DEFINITION -----	64
B. DESCRIPTION -----	65
C. COMPOSITING -----	67
D. STATISTICAL VALIDATION -----	71
VIII. SYNOPTIC DESCRIPTION SURROUNDING SPRING TRANSITIONS -----	74
A. 1976 (MARCH-JULY) -----	74
B. 1977 (MARCH-JULY) -----	76
IX. SEA-SURFACE TEMPERATURE ANOMALY GENERATION -----	79
A. OBSERVED ANOMALIES -----	80
B. EVALUATION METHODS -----	80
X. CONCLUSIONS -----	87
APPENDIX -----	89
BIBLIOGRAPHY -----	92
INITIAL DISTRIBUTION LIST -----	94

## LIST OF TABLES

- Table 1. Mean-monthly sea-surface temperatures (C)  
from model predictions, TRANSPAC obser-  
vations, NMFS analysis, and the estimated  
departure from normal, at two locations  
in 1976 and 1977----- 58
- Table 2. Determination of statistically different  
means of mixed layer depth, wind speed,  
and heat flux, prior to and after the  
transition day, from the composite along  
38°N in 1976----- 72

# LIST OF FIGURES

Fig. 1	Points along 175°W and 155°W, and along 38°N and 32°N, within the ADS region for which calculations were made-----	20
Fig. 2a	Observed heat content ( $10^4$ cal $\text{cm}^{-2}$ ) calculated relative to the 200 m temperature, from the TRANSPAC analysis of March 1976-----	23
Fig. 2b	Similar to Fig. 2a except for June 1976----	24
Fig. 3a	Change in heat content ( $10^4$ cal $\text{cm}^{-2}$ ) from March to June 1976. A negative value indicates June heat content exceeds March--	29
Fig. 3b	Cumulative surface heat flux ( $10^4$ cal $\text{cm}^{-2}$ ) for 15 March through 15 June 1976 computed from FNOC atmospheric prediction model. Negative values indicate net downward heat flux-----	30
Fig. 4a	Difference between cumulative heat flux and the net change in heat content for March through June 1976. Dashed lines indicate upward heat flux exceeds the net change in heat content-----	31
Fig. 4b	Cumulative surface heat flux correction field for 1976 and 1977. Dashed lines represent values added to the FNOC heat flux values (interval= $0.5$ cal $\text{cm}^{-2}$ $\text{hr}^{-1}$ )-----	32
Fig. 5a	Corrected version of Fig. 3b-----	33
Fig. 5b	Similar to Fig. 4a, except corrected cumulative heat flux field used-----	34
Fig. 6	Atmospheric forcing from 15 March to 15 July 1976 at 38°N, 135°W including wind speed ( $\text{m s}^{-1}$ ), total heat flux ( $\text{cal cm}^{-2}$ $\text{hr}^{-1}$ ), and solar radiation ( $\text{cal cm}^{-2}$ $\text{hr}^{-1}$ )-----	36
Fig. 7	Similar to Fig. 6, except at 38°N, 155°W---	37

Fig. 8	Predicted mixed layer temperature (top) and depth (bottom) changes, relative to initial values on 15 March 1976, at points along 38°N. Longitude 225 corresponds to 135°W and each 10° longitude corresponds to 2C change in temperature or 100 m change in depth-----	42
Fig. 9	Predicted mixed layer depth changes, relative to an initial depth (1 m) on 15 March 1976, at points along 155°W. Each 2° latitude corresponds to 100 m change in depth-----	45
Fig. 10	Similar to Fig. 9, except for predicted mixed layer temperature changes. Each 2° latitude corresponds to 2C change in temperature-----	48
Fig. 11	Mean-monthly temperature profiles in 10 m intervals at 38°N, 155°W (left) and 38°N, 135°W (right) for Spring 1976: March (circles), April (triangles), May horizontal dashes), and June (crosses). TRANSPAC analysis values for June (diamonds) for verification-----	51
Fig. 12	Similar to Fig. 6, except at 46°N, 155°W in 1976-----	54
Fig. 13	Similar to Fig. 6, except at 46°N, 155°W in 1977-----	56
Fig. 14	Similar to Fig. 11, except at 46°N, 175°W (left) and 46°N, 155°W (right) for Spring 1977-----	57
Fig. 15	Similar to Fig. 11, except for Spring 1977 at 38°N, 175°W with unmodified values (left) and reduction of heat flux by 10 cal cm <sup>-2</sup> hr <sup>-1</sup> (right)-----	61
Fig. 16	Predicted mixed layer depth changes at 30°N and 32°N along 175°W for (a) unmodified values, (b) 5 cal cm <sup>-2</sup> hr <sup>-1</sup> , and (c) 10 cal cm <sup>-2</sup> hr <sup>-1</sup> reduction of heat flux. 2° latitude corresponds to a 100 m change in depth	62
Fig. 17	Spring transition dates (Julian) for the sampled locations within the ADS area for 1976 and 1977-----	66

- Fig. 18a Composite of model-predicted mixed layer temperature (upper) and depth (lower), for 6 locations along  $38^{\circ}\text{N}$  in 1976, relative to the transition dates (day 0). Upper composite displays the deviation of temperature ( $^{\circ}\text{C}$ ), with respect to the mean temperature of the 30-day record----- 69
- Fig. 18b Composite of atmospheric forcing parameters for 6 locations along  $38^{\circ}\text{N}$  in 1976, relative to the transition dates (day 0)----- 69
- Fig. 19 Sea-level pressure patterns within the ADS area reproduced from the FNOC North Pacific analyses. Transition locations (marked by X's) for Julian days 99, 124, and 163 in 1977----- 78
- Fig. 20 Difference in mixed layer temperature (1976 minus 1977) at points along  $38^{\circ}\text{N}$  with positive values enclosed in envelope and negative values in dotted regions. Transition dates: 1976 (circle), 1977 (cross). Each  $10^{\circ}$  longitude corresponds to  $3.1^{\circ}\text{C}$ ----- 82
- Fig. 21 Difference between the transition date versus the net accumulated temperature increase ( $^{\circ}\text{C}$  days) from the earlier transition date (1976 or 1977) to day 195 for all locations shown in Fig. 1----- 85

## ACKNOWLEDGEMENTS

The author would like to thank Drs. Warren White and Steve Pazan of NORPAX for providing oceanic data and FNOG atmospheric forcing fields. At the Naval Postgraduate School, Pat Gallacher provided programs for data handling, assisted the author in using them, and offered comments on the manuscript. Professor Bill Garwood provided the ocean mixed layer prediction model and also read the manuscript. The computing was done at the W. R. Church Computer Center.

The author would like to express sincere gratitude to Professor Russ Elsberry for his guidance during research and preparation of this thesis.

Acknowledgement for sponsorship goes to the National Oceanic and Atmospheric Administration and the National Weather Service who granted the scholarship which made possible the author's attendance at the Naval Postgraduate School.

## I. INTRODUCTION

### A. HYPOTHESIS

One aspect of the large-scale variability in the ocean thermal structure is the seasonal transition of the depth of the upper ocean layer. During the spring, the ocean mixed layer transforms from a deep winter regime to a shallow summer regime. Following this change in the depth of the mixed layer is a subsequent increase in the temperature of the mixed layer.

If the transition between the winter and summer regimes occurs earlier (later) than normal, the seasonal heating is expected to be accumulated in a shallow (deep) layer and will tend to produce a positive (negative) sea-surface temperature (SST) anomaly. This hypothesis has been tested [Elsberry and Garwood, 1978] at Ocean Weather Ship (OWS) "P" (50°N, 145°W). For this study, it was tested over a wide areal extent, with emphasis on determining relations to large-scale SST anomalies being investigated in the North Pacific Experiment (NORPAX). The study was based on the principle that the changes in the structure of the seasonal pycnocline, are primarily a result of vertical mixing processes in response to atmospheric forcing [Elsberry and Garwood, 1978].

### B. BACKGROUND

There are at least two dominant time scales governing the time-varying generation of oceanic turbulence. The



passage of atmospheric storms is the time scale with the longer (synoptic) period, while the daily heating cycle is the shorter (diurnal) period time scale.

### 1. Synoptic Time-Scale

During the passage of atmospheric storms, upward surface heat flux to the atmosphere may result in significant cooling of the upper ocean. During the fall, a significant fraction of the seasonal sea-surface temperature reduction takes place when wind-generated turbulence and convective overturning, in the upper ocean during atmospheric storms, mix into the stable thermocline layer [Elsberry and Camp, 1978]. The strongest oceanic response to atmospheric storms is produced early in the fall, when a shallow and warm mixed layer exists. Late in the fall when the mixed layer is deep, strong forcing events have a much diminished effect. An above (below) normal number of storms is correlated with anomalously low (high) sea-surface temperature during the cooling season [Elsberry and Camp, 1978].

Much of the oceanic response to the passage of an extra-tropical cyclone can be described in terms of one-dimensional processes, or non-advective, mixed layer dynamics. The significant changes in the mixed layer depth and temperature are well correlated with the amplitude and timing of the atmospheric forcing [Camp and Elsberry, 1978].

### 2. Diurnal Time-Scale

Daytime heating from solar radiation is mainly absorbed

in the upper ten to twenty meters, producing a layer of less dense water near the surface. When turbulence is insufficient to transport the accumulated heat to an established mixing depth, a shallowing of the mixed layer occurs. The stable layer, formed during the period of maximum daytime heating, is eroded during the night by convective turbulence associated with the upward heat flux, and by mechanical mixing due to the wind.

The depth over which the daytime heating is distributed is primarily determined by the amount of wind stirring, which is a function of the frequency and intensity of atmospheric storms. The diurnal variation in the mixed layer depth, after the seasonal thermocline has been established, is only a fraction of the variation that occurs prior to the formation of the thermocline. The diurnal heating cycle during late winter can cause the mixed layer depth to vary between nighttime depths of 100-150 meters and daytime depths of 10-40 meters [Elsberry and Garwood, 1978].

### 3. Atmospheric Friction Velocity ( $u_*$ )

The importance of specifying correctly the high wind speed events for predicting sea-surface temperature changes is documented by Elsberry and Raney (1978). The values of the atmospheric friction velocity ( $u_*$ ), were calculated from observations at ocean weather ships in the Pacific. Since the wind generation of mechanical energy is proportional to  $u_*^3$ , the distribution of  $u_*^3$  was calculated for OWS "V"

(34°N, 164°E) from January to August 1959. The daily values of  $u_*^3$  were shown to have a marked decrease after the middle of March, with small values continuing throughout the summer.

The most consistent result, as reported by Elsberry and Raney (1978), was in the duration of the high wind speed events. These events occurred 35-37 percent of the time, regardless of the season, and contained about 70 percent of the total  $u_*^3$ . The fact that a major fraction of the mechanical generation of turbulent kinetic energy in the upper ocean occurs during such a limited period of stronger winds, is important for understanding the resulting changes in thermal structure. Low values of  $u_*^3$  were associated with sea-surface temperature increases during the warming season. The association between those events emphasized the role of vertical mixing in the redistribution of the heat absorption.

#### 4. Spring Transition

The transition from a winter mixed layer regime to a summer regime occurs during the spring, when the net daily insolation values are increasing, and the occurrence of high wind speed events is diminishing. The increasing solar radiation, which is predominately absorbed in the near-surface layer, tends to promote stability. The more stable the layer, the better it resists the eroding effects of the mixing generated during high wind periods.

Tully and Giovando (1963) noted that the spring transition appeared to be rapid. Elsberry and Garwood (1978)

have reported that their modeling studies showed that the transition can take place in a single diurnal cycle. The key synoptic feature initiating the transition, as reported by Elsberry and Raney (1978), was an extended interval of weak winds coinciding with a period of net downward heat flux. A layer of warmer and less dense water near the surface was established with the retreat of the mixed layer during the daytime heating period. If the mechanical generation of turbulent kinetic energy was sufficiently small, the stable layer remained intact through the subsequent night. A repetition of this cycle for several days, would likely lead to the establishment of the seasonal thermocline.

#### 5. Development of SST Anomalies

After the spring transition, the mixed layer is confined to a much shallower zone. Consequently, the rate of heat accumulation within the layer is much greater, and the temperature will rise appreciably, if the layer is undisturbed for a few days. Elsberry and Garwood (1978) have suggested that the predominance of anomalously high or low sea-surface temperature patterns, at some locations, can be explained in terms of the limiting depth over which the incoming heat flux is distributed. In their study, the anomalous sea-surface temperature at OWS "P" (50°N, 145°W), averaged over March through December, was plotted as a function of the transition date. The hypothesis of an earlier than normal transition date leading to an early beginning of the seasonal warming,

and thus, to a consistently higher than normal sea-surface temperature, appeared to be verified for that sample.

During and after the formation of the seasonal thermocline, an increase in sea-surface temperature would tend to be negated by the heat and momentum fluxes associated with a strong atmospheric storm. That is, a decrease in sea-surface temperature is found during periods of higher wind speeds, as the surface layer heat is redistributed by vertical mixing. The observed sea-surface temperature increase during the heating season is, therefore, a balance between the greater increases during low wind periods, and the small decreases that occur during high wind periods [Elsberry and Raney, 1978].

Anomalous solar radiation (an extended cloudy period or many cloud-free days) or anomalous redistribution of the upper layer heat, can cause anomalous sea-surface temperatures. The anomalous solar radiation does not appear to be a primary factor. Elsberry and Raney (1978) found that the increases in sea-surface temperature at the ocean weather ship locations were better associated with sustained periods of low wind speeds, than with periods of above normal insolation.

The anomalous vertical redistribution of heat in the upper ocean is probably caused by anomalous heat flux at the surface, or anomalous entrainment heat flux at the mixed layer base generated by wind stirring and convective over-turning [Elsberry and Garwood, 1978]. Other processes, which are

non-local and not evaluated in this study, are the horizontal divergence of the surface layers produced by wind stress curl, and the horizontal advection produced by surface Ekman flow.

### C. STUDY DESCRIPTION

The Anomaly Dynamics Study [ADS, 1978] area of NORPAX was the oceanic region studied (Fig. 1). The largest thermal variability in the mid-latitude Pacific occurs between  $30^{\circ}\text{N}$ - $50^{\circ}\text{N}$  and  $140^{\circ}\text{W}$ - $180^{\circ}\text{W}$  within the ADS area, which is also a region of strong atmospheric variability. Points at  $10^{\circ}$  longitude intervals along  $38^{\circ}\text{N}$  and  $32^{\circ}\text{N}$  from  $175^{\circ}\text{E}$  to  $135^{\circ}\text{W}$  were sampled. Points at  $2^{\circ}$  latitude intervals along  $175^{\circ}\text{W}$  and  $155^{\circ}\text{W}$  from  $30^{\circ}\text{N}$  to  $50^{\circ}\text{N}$  were also chosen. This provided a representative set of locations from which inferences about the large-scale oceanic variability were made. Locations along  $32^{\circ}\text{N}$  were chosen for additional analysis of a suspected discrepancy in the heat flux fields near the southern boundary.

The one-dimensional or vertical mixing process was represented through the Garwood (1977) oceanic mixed layer model. The model required atmospheric forcing fields of wind, solar radiation, and surface heat flux on time scales of hours, because of the necessity of resolving the diurnal response in the ocean. This diurnal component can modulate the seasonal trend [Garwood, 1977]. The model was supplied with an initial temperature profile for a given month and location.

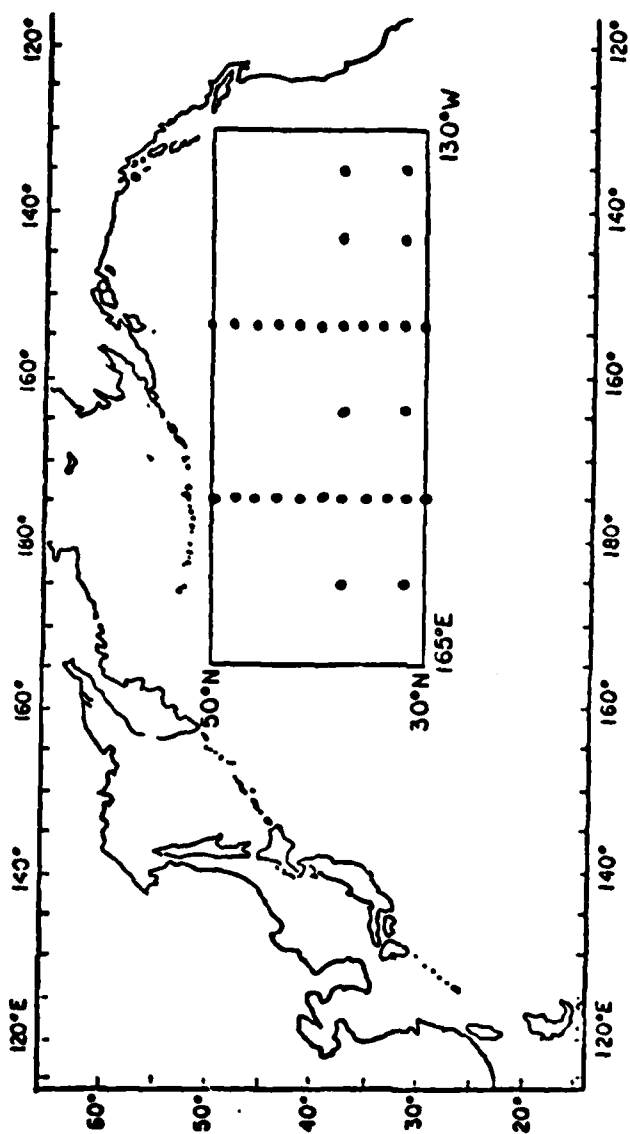


Fig. 1 Points along 175°W and 155°W, and along 38°N and 32°N, within the ADS region for which calculations were made.

It then predicted the evolution of the oceanic thermal structure, caused by surface processes alone, at a geographical location for a specified period of time.

Values of wind speed, solar radiative flux, and total surface heat flux were extracted from the Fleet Numerical Oceanography Center (FNOC) historical data files of the atmospheric predictions and analyses. The east and west wind components were available at 6-hour intervals, and the solar and total surface heat (latent plus sensible plus back radiation minus solar) flux values were at 12-hour intervals. To resolve properly the oceanic response to the diurnal heating cycle, surface forcing values had to be provided at hourly intervals. A complete description of the procedures and programs for performing the data manipulation, from editing to interpolating the forcing fields, is available in Gallacher (1979). An abbreviated description of the system programs is provided in the appendix.



## II. COMPARISON OF HEAT CONTENT WITH CUMULATIVE SURFACE HEAT FLUX

### A. HEAT CONTENT

The one-dimensional, mixed layer model considered only the vertical fluxes of heat. Therefore, a necessary (but not sufficient) condition for acceptable predictions was that cumulative surface heat flux, as used by the model, be similar to the observed ocean heat content change. This condition had to be met before the model-generated results could be effectively evaluated.

The observed heat content of a column of water at grid points within the ADS area was calculated using trapezoidal integration. To minimize the effects of any horizontal processes that were present, the heat content was computed relative to the temperature at 200 meters. Optimally analyzed TRANSPAC BTs at 0, 30, 60, 90, 120, 150, and 200 meters at monthly intervals from March to June of 1976 and 1977, were used as data [White and Bernstein, 1979].

The observed heat content pattern for March 1976 is depicted in Fig. 2a. The greater heat content was located in the southeastern portion, while the smaller amounts were found in the northwest. There was significant increase in the heat content from west to east. A negative heat content frequently occurred in the northern latitudes during late winter and

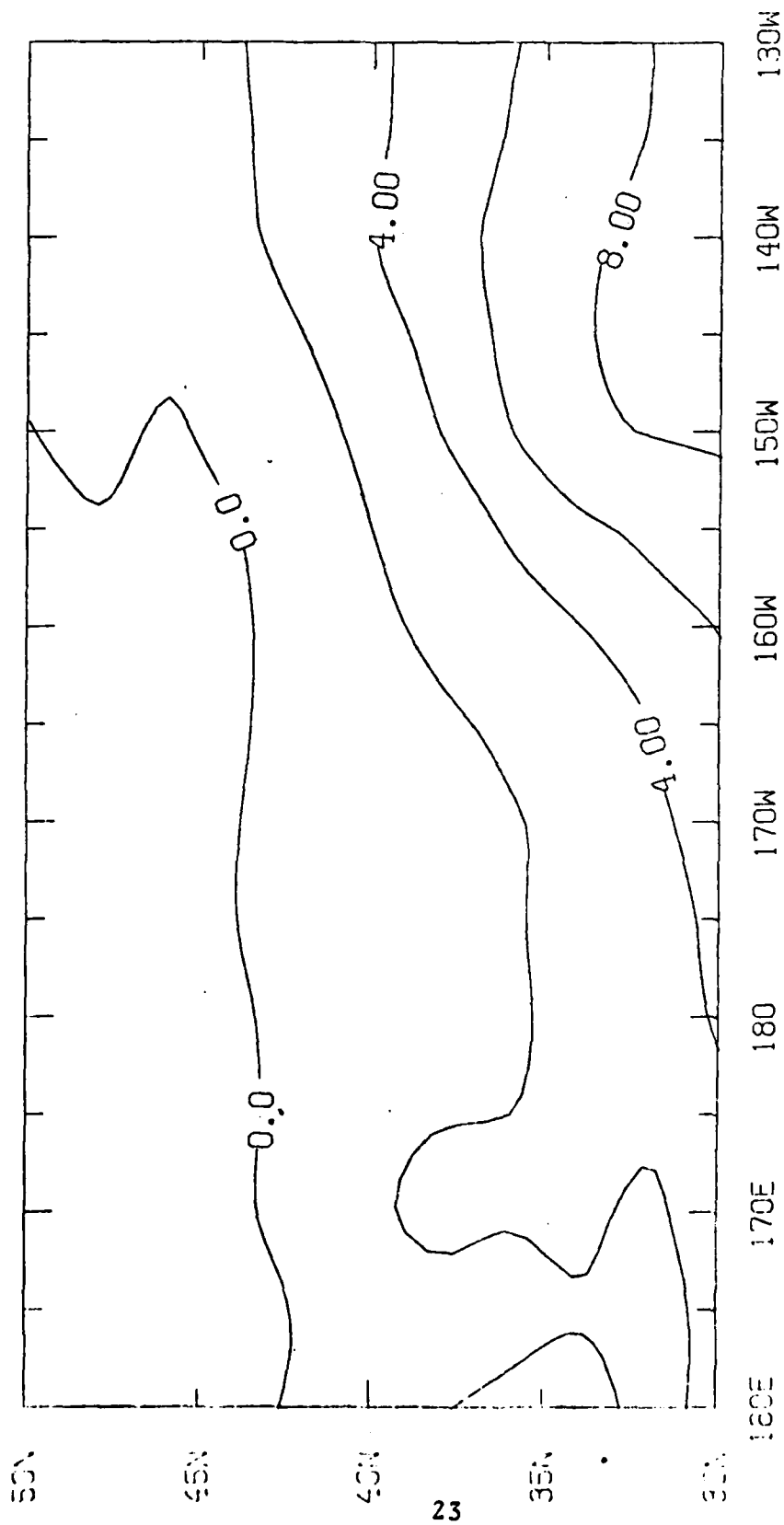


Fig. 2a Observed heat content ( $10^4 \text{ cal cm}^{-2}$ ) calculated relative to the 200 m temperature, from the TRANSPAC analysis of March 1976.

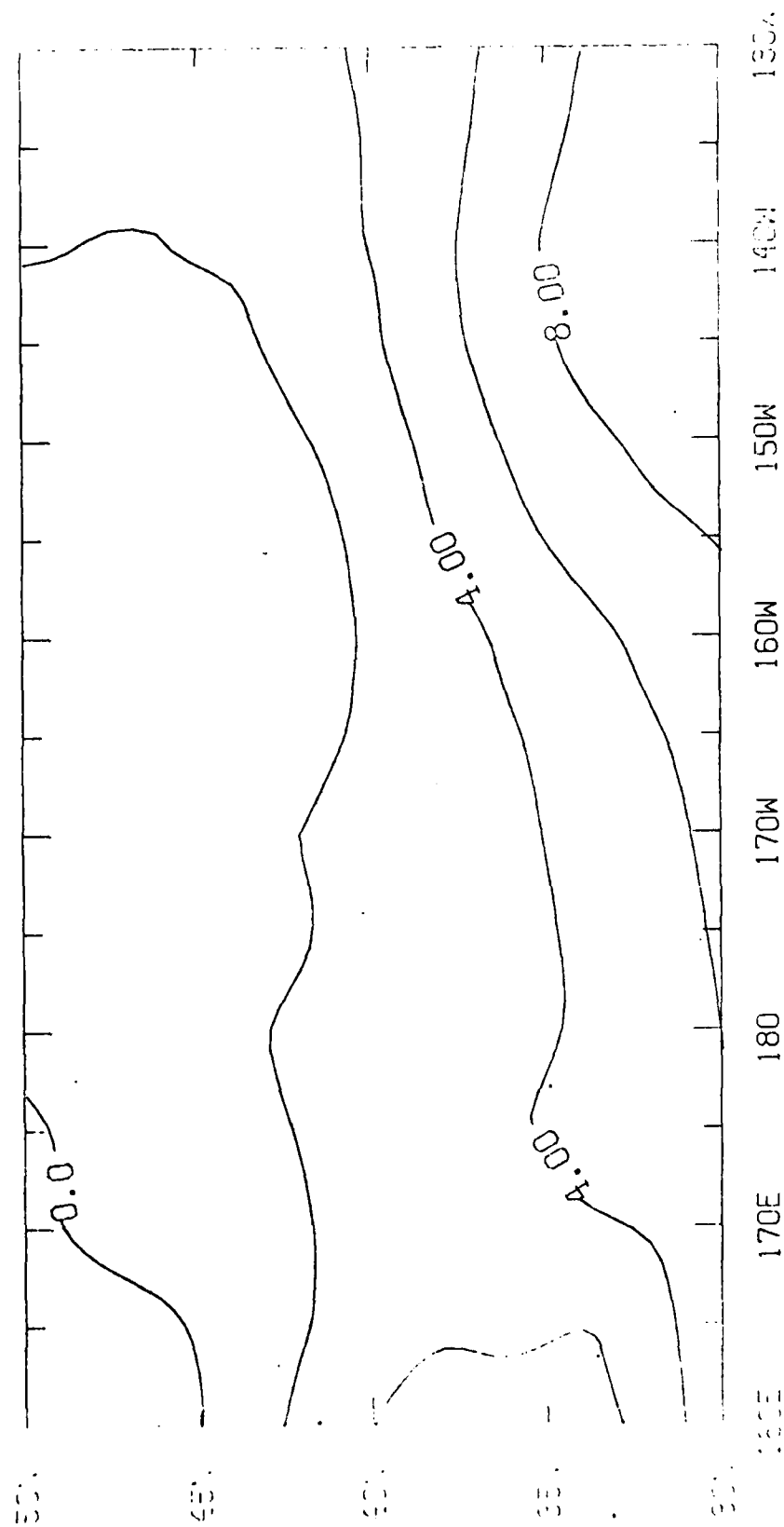


Fig. 2b Similar to Fig. 2a except for June 1976.

early spring. This negative value meant the temperature profile was warmer with increasing depth, rather than colder. The highest heat contents in the southeastern portion were related to higher near-surface temperatures, and to lower 200-meter temperatures, than those of other regions. This situation allowed a steeper than normal thermocline down to 200 meters, which supported a stable water mass. This stable temperature structure was shown to be closely related to a persistent atmospheric high pressure area over that region.

The heat content of June 1976 (Fig. 2b) demonstrated the response of the ocean to three months of the heating season. There was much less longitudinal variability in June than in March, which was partially attributable to a slackening of surface wind strength over this period. As shown in Fig. 3a, larger heat content gain was realized in the western part ( $20,000\text{--}30,000 \text{ cal cm}^{-2}$ ) than in the eastern part ( $7,500\text{--}10,000 \text{ cal cm}^{-2}$ ). A negative difference in the March minus June heat content corresponds to the net ocean heat gain during this period.

In 1977 (not shown), the heat content of the North Pacific in March and June had a remarkable similarity in pattern to Fig. 2, in spite of the vastly different atmospheric wind regimes that existed. In March, the southeastern region of the ADS area had the highest heat content as in the previous year, but the values were not as great. By June, though, the heat content of the western portion had risen substantially

(20,000-30,000 cal cm<sup>-2</sup>) over that of the far eastern portion (7,500-15,000 cal cm<sup>-2</sup>). In both years, the northern portion of the ADS area exhibited a greater increase in heat content, from March to June, than the southern portion. Considering the entire ADS area, the 1977 heat contents were less than those of 1976.

#### B. CUMULATIVE HEAT FLUX

The daily surface heat flux values estimated from the FNOG fields were interpolated to hourly intervals, and then accumulated for a 92-day period from March 15 to June 15. This period roughly corresponded to the March to June heat content change. Negative values in Fig. 3b indicate downward surface heat flux, which tends to warm the upper ocean layer, whereas, positive values indicate a loss of heat. An unrealistic pattern developed over the southern latitudes. Due to the increased solar flux that is expected over this region during this period, a net downward heat flux of similar or greater values than those of the northern latitudes should have been realized. This discrepancy is shown in Fig. 4a, which is the difference between the cumulative heat flux and the net change in heat content over the three-month period. This field has been filtered to remove short-wavelength features. A negative value (dashed lines) indicates that more downward, or less upward, cumulative heat was required for parity. There was reasonable agreement in the vicinity of 38°N and 40°N and north of 46°N

latitude. Between these two regions was an area of excessive downward heat flux. This area is near the ocean polar front, where the strong north-south temperature gradient might have supported widely varying heat content values. South of 38°N, there was a steady increase in the difference to as much as 30,000 cal cm<sup>-2</sup> for the period. This excessive upward heat flux is probably linked with a systematic bias in the surface heat flux calculations provided by FNOC. However, a portion of this discrepancy may be due to errors in the estimates of the heat content change deduced from the TRANSPAC analyses. If the anomalous values near the southern boundary in Fig. 4a are attributable to the FNOC surface heat fluxes, it may affect ocean prediction models that use these forcing fields. While the surface fluxes are of primary importance for long-term ocean modeling, they are of secondary importance in atmospheric models [Gallacher, 1979].

### C. ADJUSTMENTS TO HEAT FLUX

The heat flux bias was suspected at an early stage in the study, but was not confirmed until interpretations were made over the entire ADS area. Corrections that were uniform in time and smoothly varying in space were then applied to the heat flux fields, and the ocean model results were re-evaluated to determine the effects of the adjustments. The corrections were made by using the filtered bias field as in Fig. 4a for 1976, and a similar field for 1977. These fields were averaged

to form the correction field which was applied uniformly in time during both years.

The correction field that was used to adjust the interpolated surface heat fluxes on an hourly basis over the 3-month period is shown in Fig. 4b. The pattern of positive and negative values was similar to Fig. 4a. The corrected version of the integrated surface heat flux for 1976 is shown in Fig. 5a. A closer correlation between surface heat flux (Fig. 5a) and the observed heat content change (Fig. 3a) was achieved using the correction field in Fig. 4b.

Successful reduction of the systematic bias is evident in the difference between the surface heat flux and the heat content change, as in Fig. 5b. There are small areas that are not in close agreement, especially around 170°E. All values to the west of 170°E during 1976 were fictitious, and were not used in this work. The remainder of the differences were attributable to a number of factors besides the bias in cumulative heat fluxes. There were physical processes, notably horizontal advection, not taken into account by the one-dimensional requirement for local heat balance. For instance, the discrepancy along 170°E in Fig. 5b may have been associated with proximity to the Kuroshio extension. The interpolated BT analyses may have been somewhat less accurate near the southern boundary, due to a lack of ship-of-opportunity reports in that region. There were also residual errors in the computation of the heat content of each grid point, which used trapezoidal integration with respect to 200 meters.

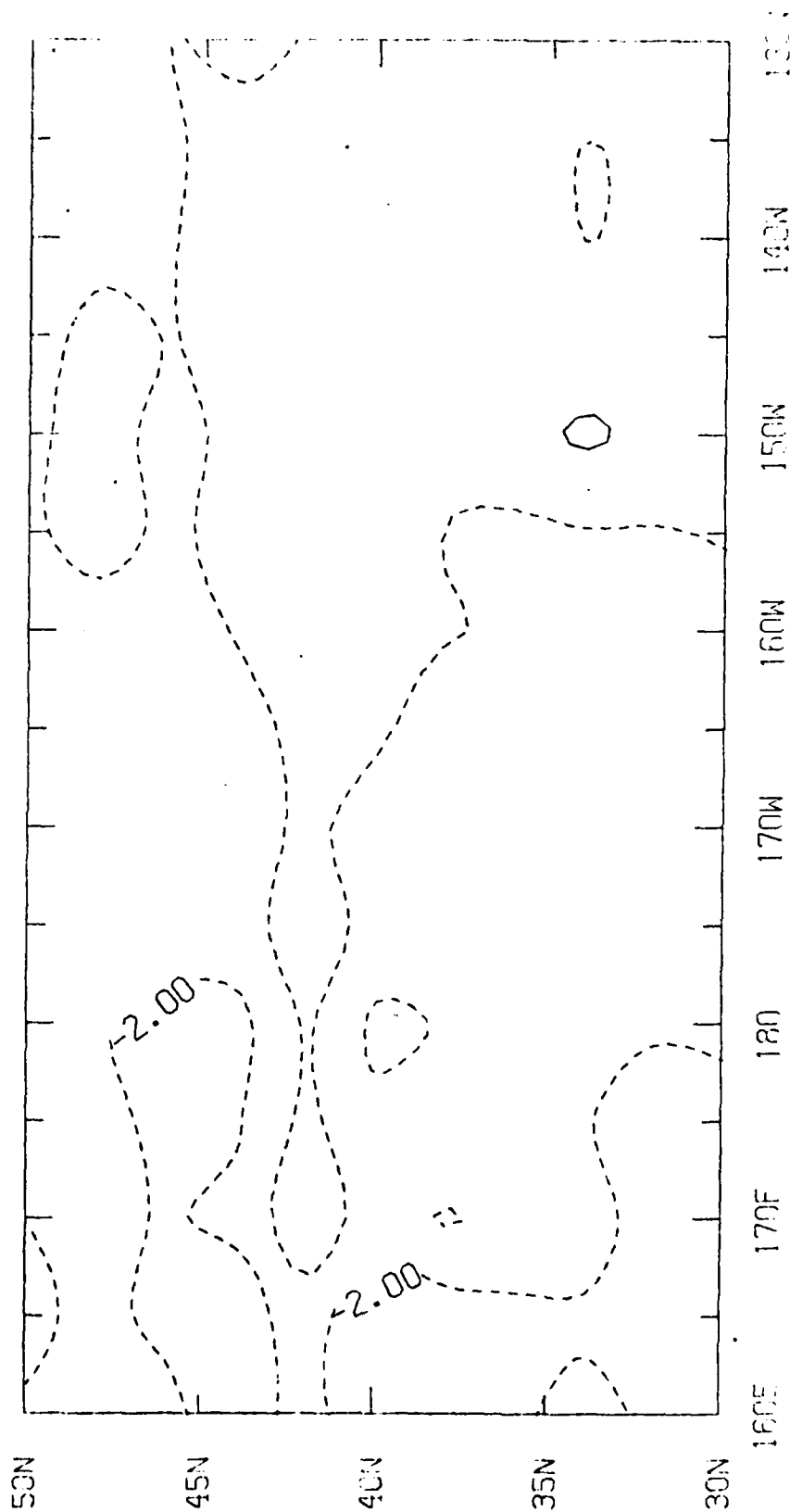


Fig. 3a Change in heat content ( $10^4 \text{ cal cm}^{-2}$ ) from March to June 1976. A negative value indicates June heat content exceeds March.



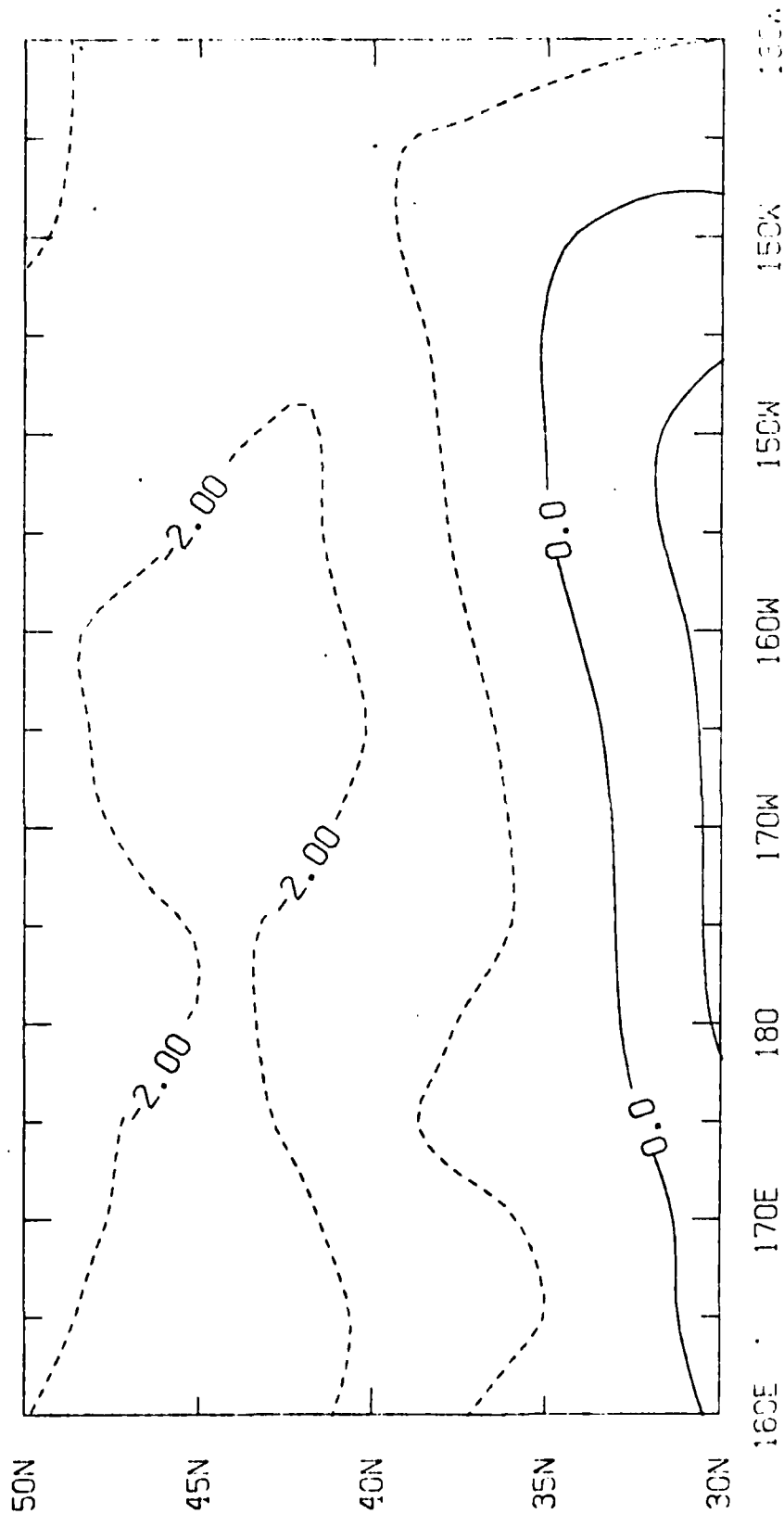


Fig. 3b Cumulative surface heat flux ( $10^4 \text{ cal cm}^{-2}$ ) for 15 March through 15 June 1976 computed from FNOG atmospheric prediction model. Negative values indicate net downward heat flux.

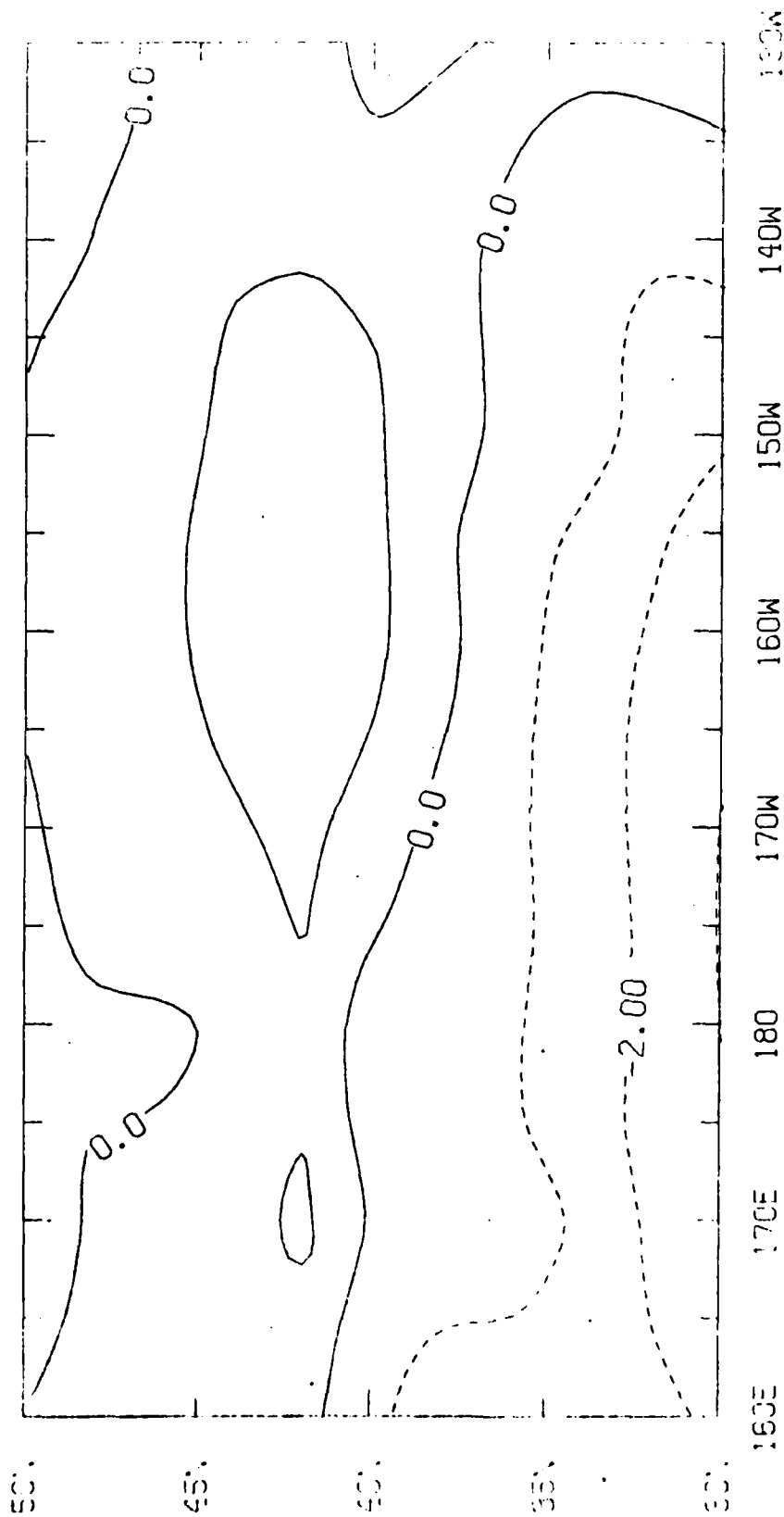


Fig. 4a Difference between cumulative heat flux and the net change in heat content for March through June 1976. Dashed lines indicate upward heat flux exceeds the net change in heat content.

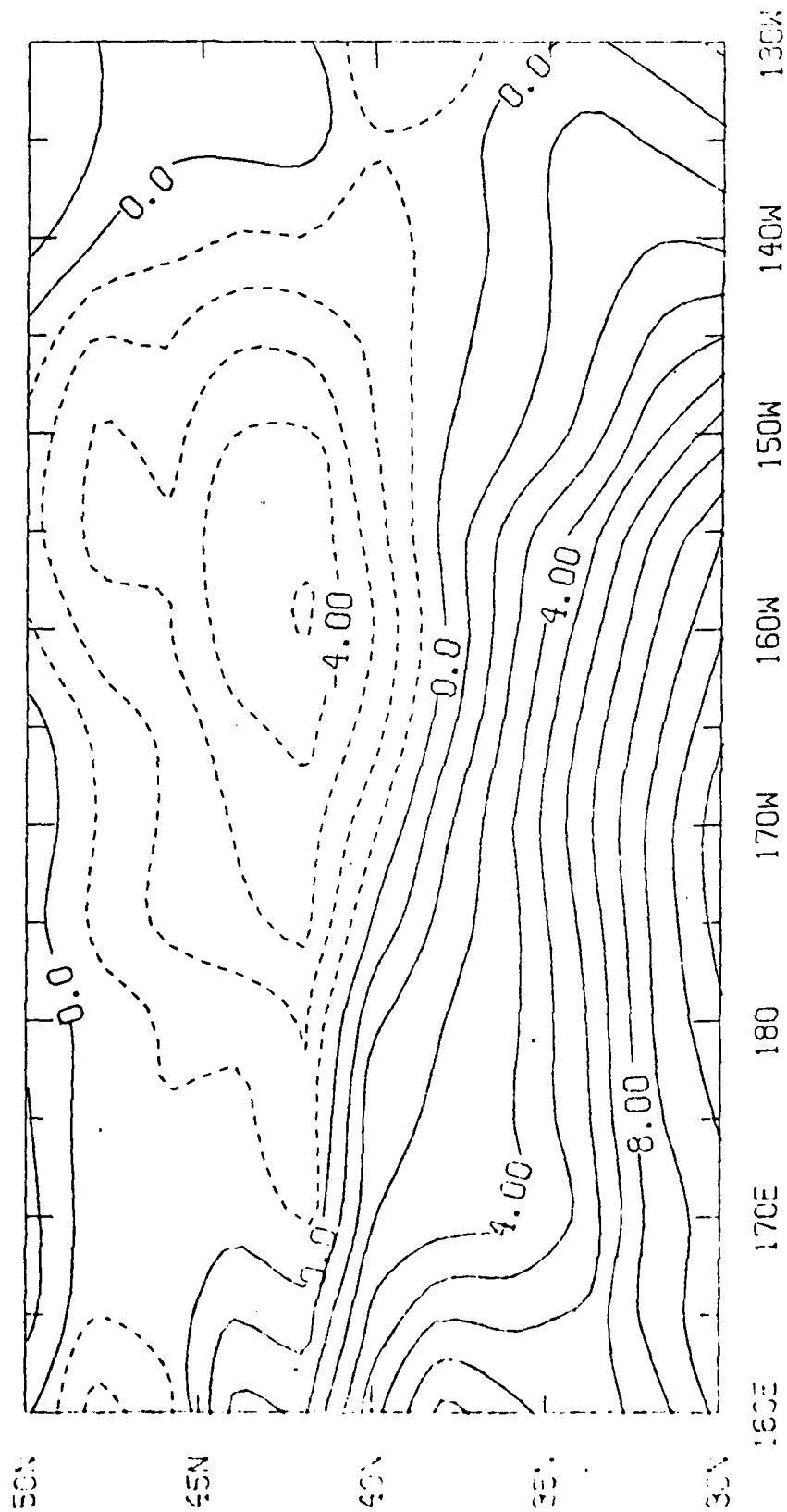


Fig. 4b Cumulative surface heat flux correction field for 1976 and 1977. Dashed lines represent values added to the FNOc heat flux values (interval=0.5 cal cm<sup>-2</sup>hr<sup>-1</sup>).

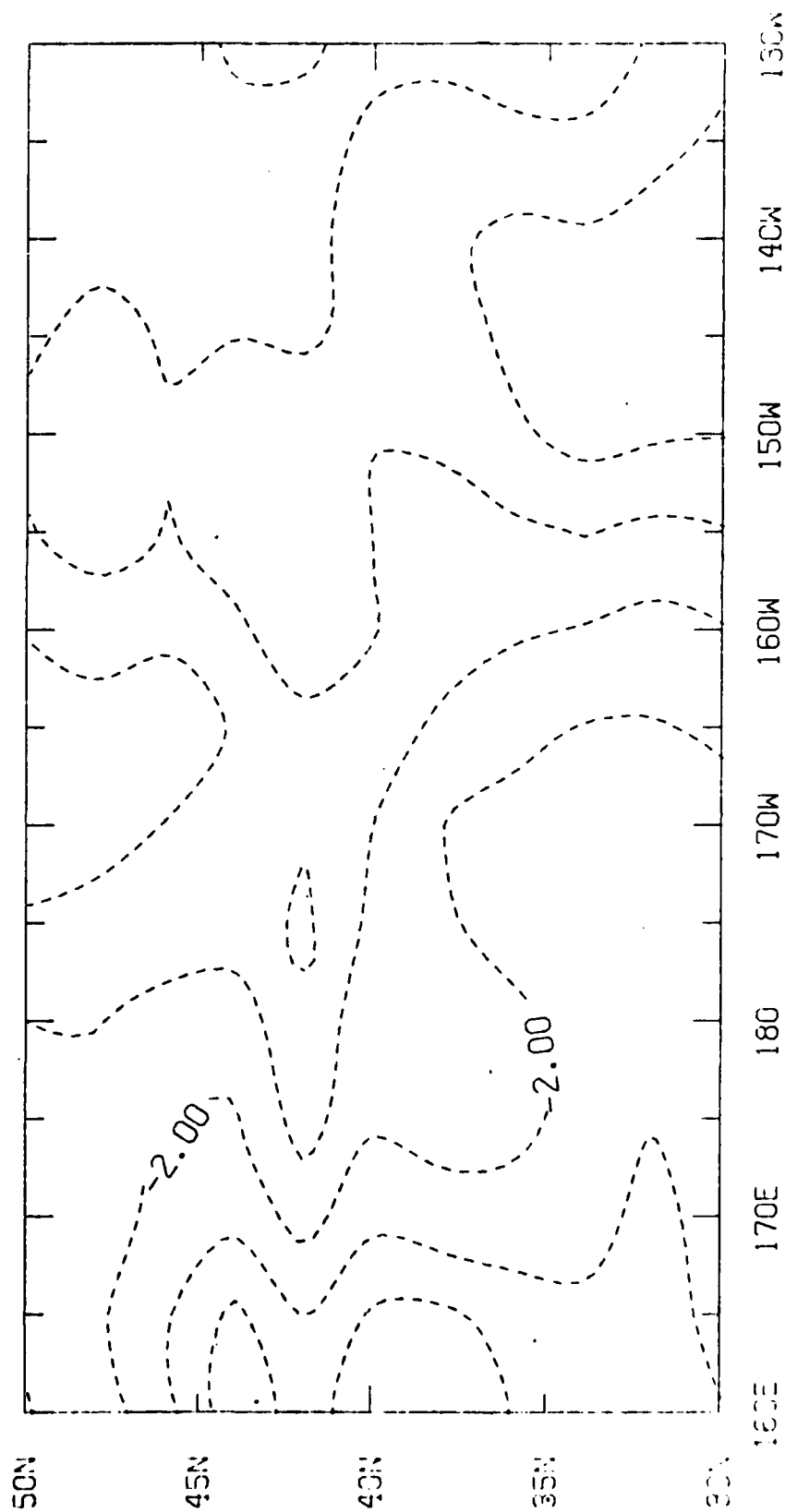


Fig. 5a Corrected version of Fig. 3b.

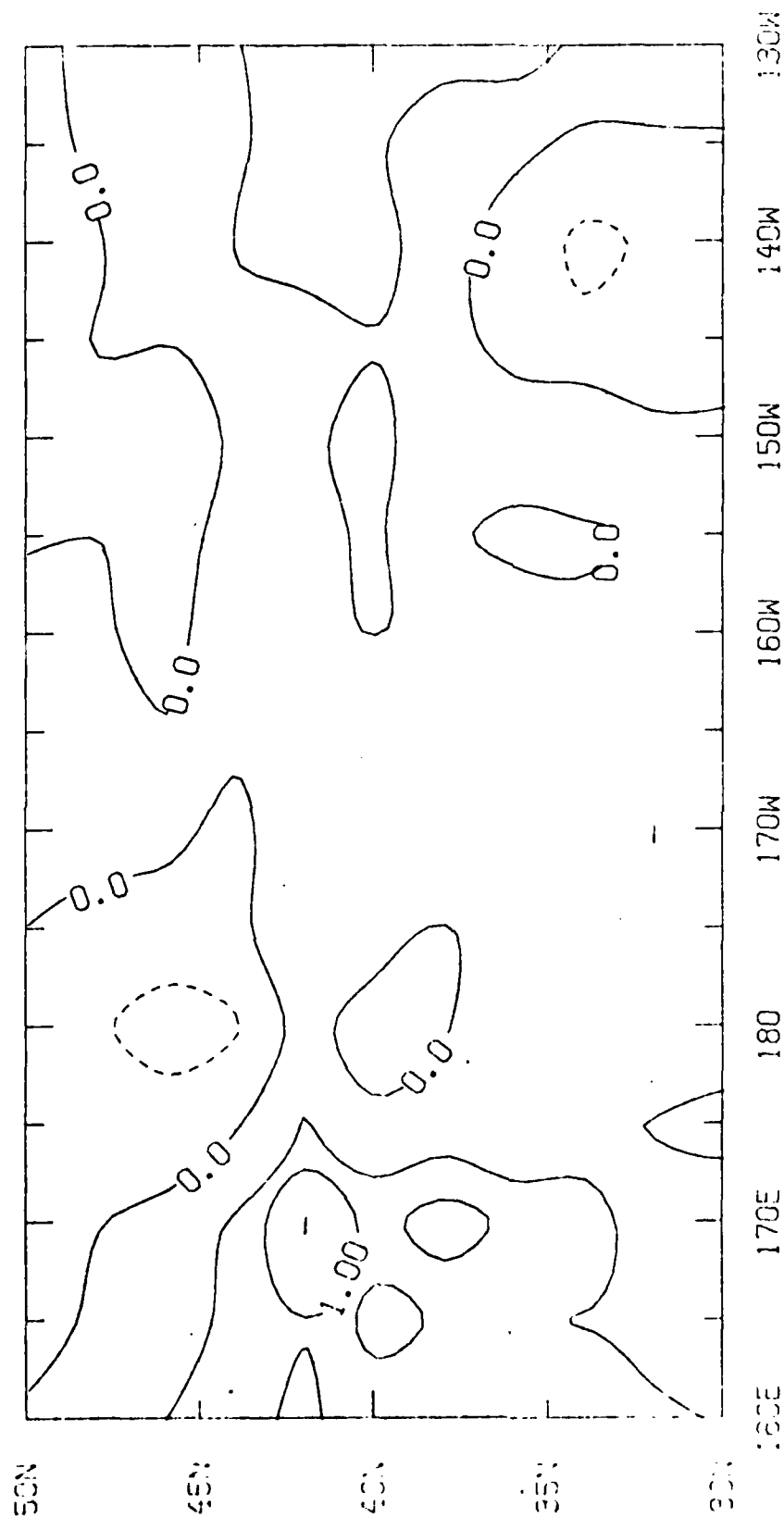


Fig. 5b Similar to Fig. 4a, except corrected cumulative heat flux field used.

### III. TIME SERIES OF FORCING FUNCTIONS

For all the locations indicated in Fig. 1, 4-month time series of hourly-interpolated wind speed, total heat flux, and solar radiation, were generated from the FNOC files. From these figures, the general development of the atmospheric parameters controlling the behavior of the upper ocean thermal structure was determined.

Time series plots for atmospheric forcing functions during spring, 1976, at  $38^{\circ}\text{N}$ ,  $135^{\circ}\text{W}$  and  $38^{\circ}\text{N}$ ,  $155^{\circ}\text{W}$  are shown in Figs. 6 and 7, respectively. The forcing at these locations exhibited dissimilar behavior, and had significantly different spring transition dates, even though they were located on the same latitude. These two locations further serve as examples of the differences and similarities in ocean structure development.

#### A. WIND SPEED

North of  $40^{\circ}\text{N}$ , the wind speed values demonstrated rapid and greater changes during the early spring, and less rapid and smaller changes later in the spring. Some peak wind speeds were in excess of 30 m/s late in March and early April. The wind speed changes displayed synoptic periodicity throughout the spring. In the southern latitudes where pressure gradients were weaker, the wind speeds were slower, steadier, and lacked

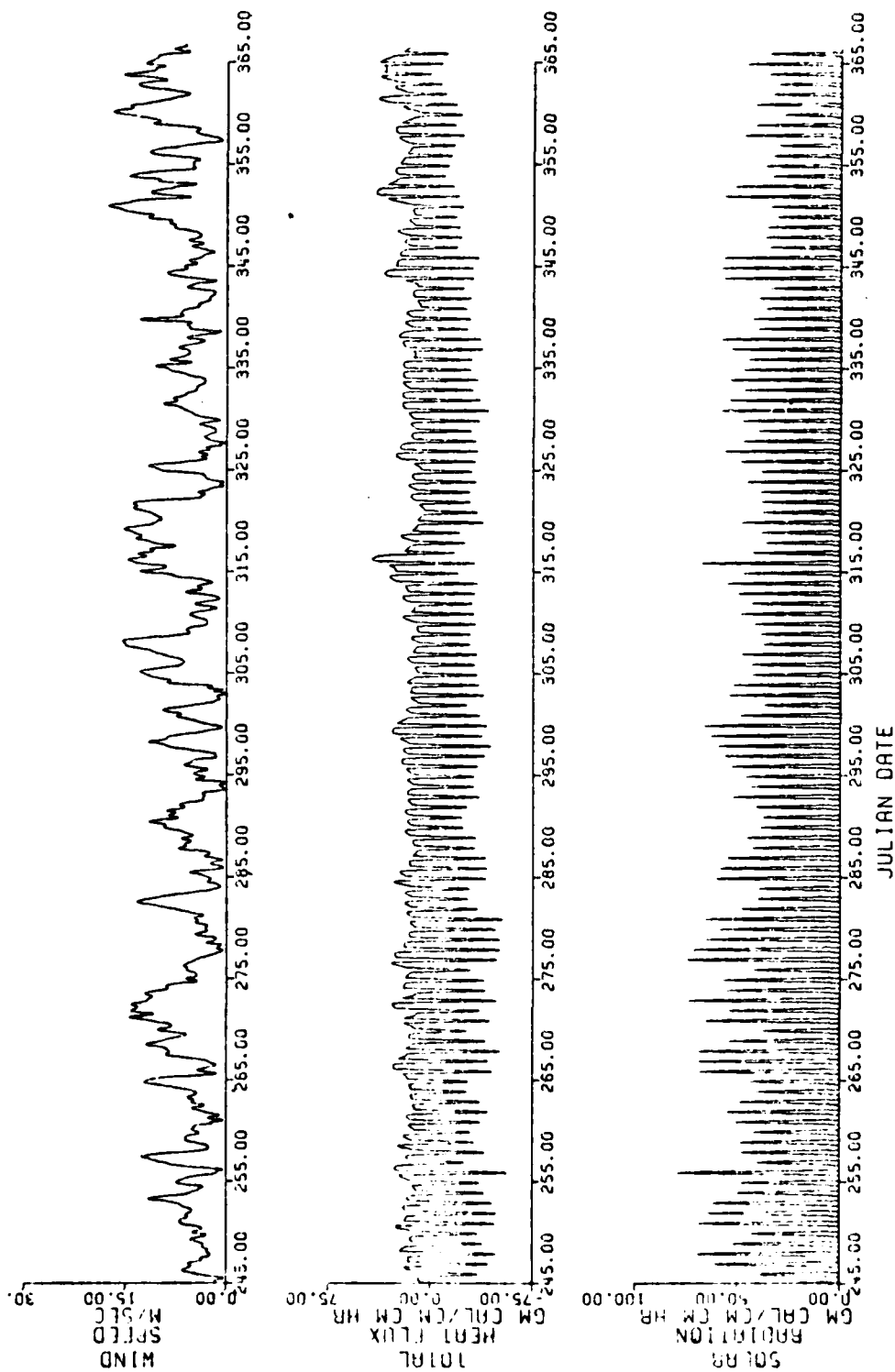


Fig. 6 Atmospheric forcing from 15 March to 15 July 1976 at 38°N, 135°W including wind speed ( $\text{m s}^{-1}$ ), total heat flux ( $\text{cal cm}^{-2} \text{ hr}^{-1}$ ), and solar radiation ( $\text{cal cm}^{-2} \text{ hr}^{-1}$ ).

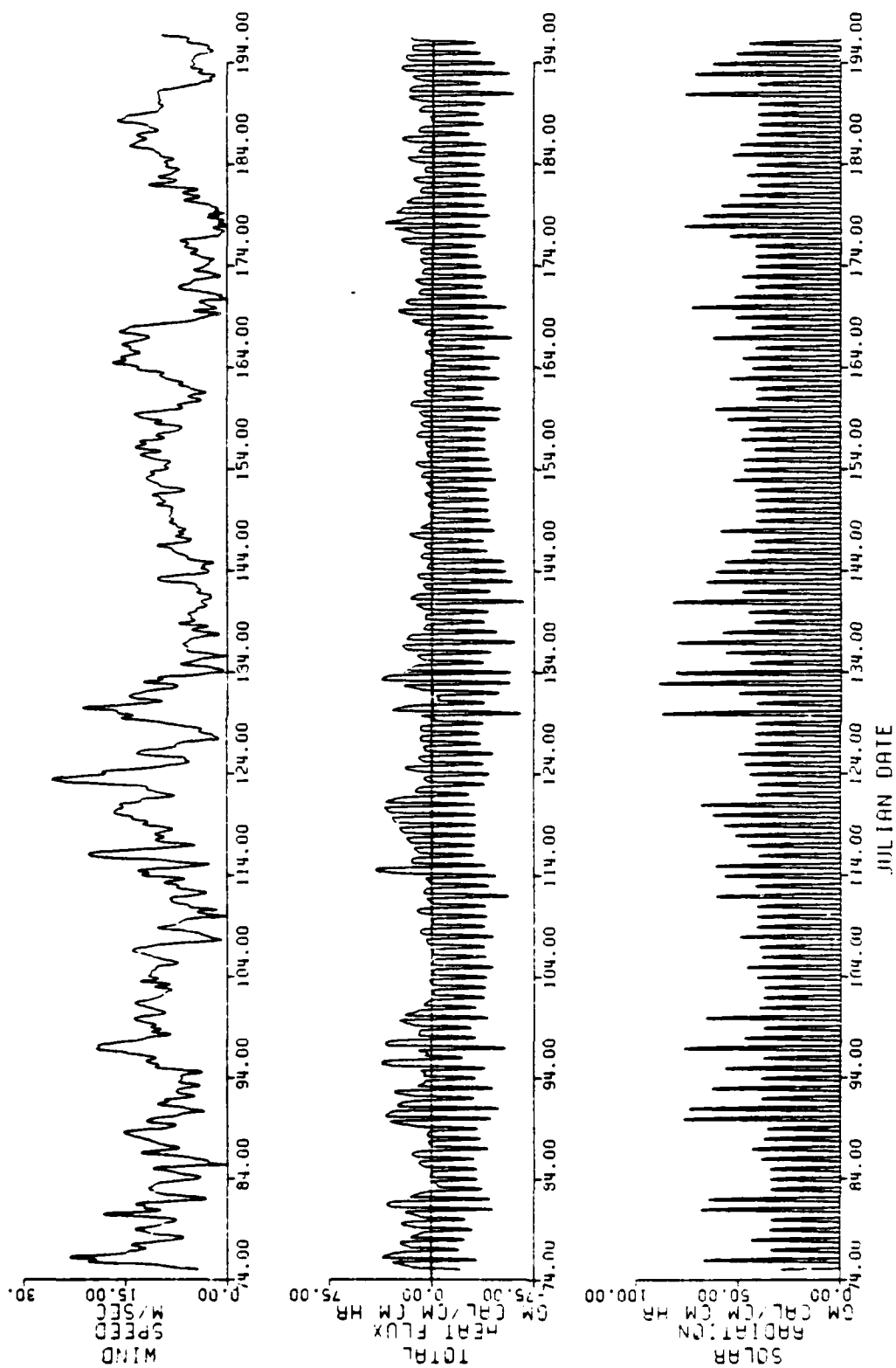


Fig. 7 Similar to Fig. 6, except at 38°N, 155°W.



the large variations that characterized the far northern time series. Later in the spring, the diurnal influence of stronger daytime winds and weaker nighttime winds became dominant, while synoptic scale variations in wind speed decreased in amplitude.

#### B. SOLAR RADIATION FLUX

The daily insolation for all latitudes and longitudes exhibited the expected increase in magnitude with the approach of the summer solstice. The synoptic variation in cloud cover was evident from the variability in the peak (local noon) values of the solar radiation time series. In the early spring, there were many instances where a period of small solar fluxes corresponded to a high wind speed event. Later in the spring, there was not much correlation between wind speed and cloud cover. In southern latitudes, there were many daily values of high solar flux in excess of  $75 \text{ cal cm}^{-2} \text{ hr}^{-1}$ .

#### C. TOTAL HEAT FLUX

The total heat flux behaved very much like its primary constituent--the solar radiation. There was increased downward heat flux with the approach of the summer solstice. During early spring periods with less solar flux and greater wind speeds, there were many intervals of strong upward flux. Some peak values were in excess of  $40 \text{ cal cm}^{-2} \text{ hr}^{-1}$ . Later in the spring, periods of zero or downward flux became common. The upward heat flux and wind speed showed a positive correlation

a majority of the time. The greatest daily upward fluxes were produced when a day with weak winds and a large amount of solar radiation was followed by rapidly increasing winds. A period of minimum solar radiation, followed by a sharp increase in the solar flux and perhaps an increase in the winds, also produced a large daily upward heat flux. These large flux values were realized because the heat content had been accumulated near the surface and was easily altered by increased wind speeds, or strong solar radiation.

The daily upward heat flux in southern latitudes displayed average values between 15 and 20 cal cm<sup>-2</sup> hr<sup>-1</sup>, and were generally higher than in northern latitudes. This characteristic was partly due to higher solar fluxes, and partly attributed to the accumulated bias discussed previously.

#### D. EXAMPLES DURING SPRING TRANSITION

With respect to the spring transition dates, the wind speed was generally high a few days prior to the transition, then the wind slackened considerably during the transition, and remained weak for the following three or four days. There seemed to have been no distinct pattern for the total heat flux, or solar flux, around transition time. The method of determining spring transition dates and compositing these forcing functions with respect to the transition date of each location is discussed in a later section.

On the transition date (day 111) in Fig. 6 a decrease in

wind speed occurred during a period of weak solar flux, and correspondingly small upward heat flux. During the following days, there was a return to steady winds and noticeably larger solar flux values. It must be noted that for days 117 through 121, the 12-hour historical values of solar flux were missing, and these were replaced by interpolated values.

The transition on day 134 for  $38^{\circ}\text{N}$ ,  $155^{\circ}\text{W}$  in Fig. 7, also showed a wind speed lull, and increased solar flux for the following days. From day 114 to 134, the winds were considerably stronger than for the same period in Fig. 6, and thus played a major role in postponing the spring transition.

Comparing the two wind speed time series, the high wind speed events were of similar intensity and had a phase lag of about a day, early in the record. After day 134, the high wind speed events were less frequent, less intense, and further out of phase. The lower solar flux periods correspond well to the increased cloudiness that would be expected during the high wind speed events. This was evident at  $38^{\circ}\text{N}$ ,  $155^{\circ}\text{W}$ , especially between days 114 and 134, when more days of weaker solar flux were shown than at  $38^{\circ}\text{N}$ ,  $135^{\circ}\text{W}$ . Despite winds of less intensity, there was greater variability in total heat flux at  $38^{\circ}\text{N}$ ,  $135^{\circ}\text{W}$ .

#### IV. OCEAN THERMAL STRUCTURE - PREDICTION/VERIFICATION

##### A. PREDICTION OF MIXED LAYER DEPTH AND TEMPERATURE

Time series of the model-generated, mixed layer depth and temperature in 3-hour increments were displayed at locations along 175°W and 155°W, and along 38°N and 32°N. Each time series was calculated separately for 122 days, and plotted relative to the initial value on March 15.

##### 1. Zonal Section

The mixed layer depth predictions along 38°N during 1976 are displayed in Fig. 8b. Time series at different longitudes are displayed along the vertical axis, with 10° longitude on the vertical axis corresponding to 100 m depth change. The six longitudes are: 175°E; 175°W (185°E); 165°W (195°E); 155°W (205°E); 145°W (215°E); and 135°W (225°E). There is a distance of 50° longitude, or about 4500 km, between the westernmost trace and the easternmost trace.

There are noticeable differences in the predicted structure of the mixed layer from west to east. At 175°E, rapid variations between deep and shallow layers are displayed in the early part, and a much smaller depth variation is shown after day 135. At 135°W, the layer transition occurred earlier, and the diurnal variability was more dominant than at 175°E. This diurnal variation is mainly the response of the mixed layer to the solar flux, as the layer deepens at night and shallows during the day.

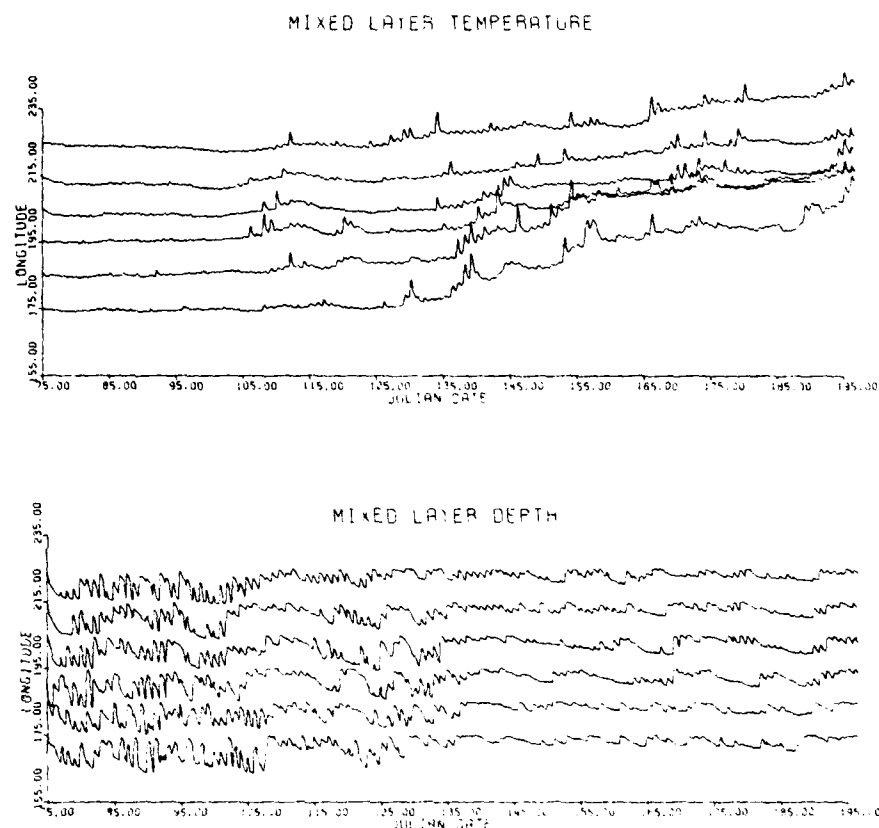


Fig. 8 Predicted mixed layer temperature (top) and depth (bottom) changes, relative to initial values on 15 March 1976, at points along  $38^{\circ}\text{N}$ . Longitude 225 corresponds to  $135^{\circ}\text{W}$  and each  $10^{\circ}$  longitude corresponds to  $2^{\circ}\text{C}$  change in temperature or  $100\text{ m}$  change in depth.

At 155°W there was sharp transition in the predicted mixed layer depth, from 82 m on day 133 at 18 GMT to 1 m on day 134 at 00 GMT. Meanwhile, at 135°W a gradual transition was predicted from day 104 at 18 GMT to day 111 at 00 GMT. At locations where there were large solar fluxes and steady winds, the mixed layer was generally more stabilized, and the transitions occurred over several daily cycles. If there was a large variation in wind speed, the transitions were only a one or two-day process. The mixed layer at 155°W stabilized after shallowing on day 109, until high wind speeds returned and deepened the mixed layer. There was another period of strong winds around day 165, which steadily deepened the mixed layer. The shallow mixed layer was sufficiently stabilized that the continued high winds could not increase it to depths typical of the winter regime.

The mixed layer temperature predictions for the same longitudes along 38°N are shown in Fig. 8a. The time series were plotted with respect to the initial surface or mixed layer temperature. Each 10° of longitude corresponded to a 2 C change in temperature. Spikes, or rapid temperature increases, in the record occurred when the mixed layer retreated to within five meters of the surface. The minimum predicted depth of one meter produced the greatest rate of increase in mixed layer temperature, especially when the shallow layer was maintained for at least six daytime hours.

A few early spikes on the traces were evident in response to prolonged shallow layer depths. Appreciable warming generally did not begin until the transition dates, which marked the establishment of a stable summer regime. The traces at 135°W and 175°E responded quite differently, even though both began with initial temperatures of 13.3 C. The warming at 175°E was significantly greater than at 135°W, in spite of only three days separating the transition dates.

In response to the spring transition at 135°W, there was a temperature jump from 13.2 C at day 111 (15 GMT), to 14.1 C on day 112 (00 GMT). For the remainder of the record, a very gradual temperature rise was predicted. At 155°W, there was a spike on day 110, but the temperature jump from 13.2 C to 14.0 C on transition day 134 marked the beginning of the stable summer regime.

Similar mixed layer behavior at 38°N and 32°N was evident at both 135°W and 175°E for both years. Along 175°E, a very shallow mixed layer after the transition date brought about large temperature increases, whereas along 135°W, a nocturnal mixed layer deepening allowed only modest temperature increases.

## 2. Meridional Section

The time series of mixed layer depths compiled at 2° latitude intervals, from 30°N to 50°N along 155°W during 1976, are exhibited in Fig. 9. All of the traces displayed a significant change in the behavior of the mixed layer depth

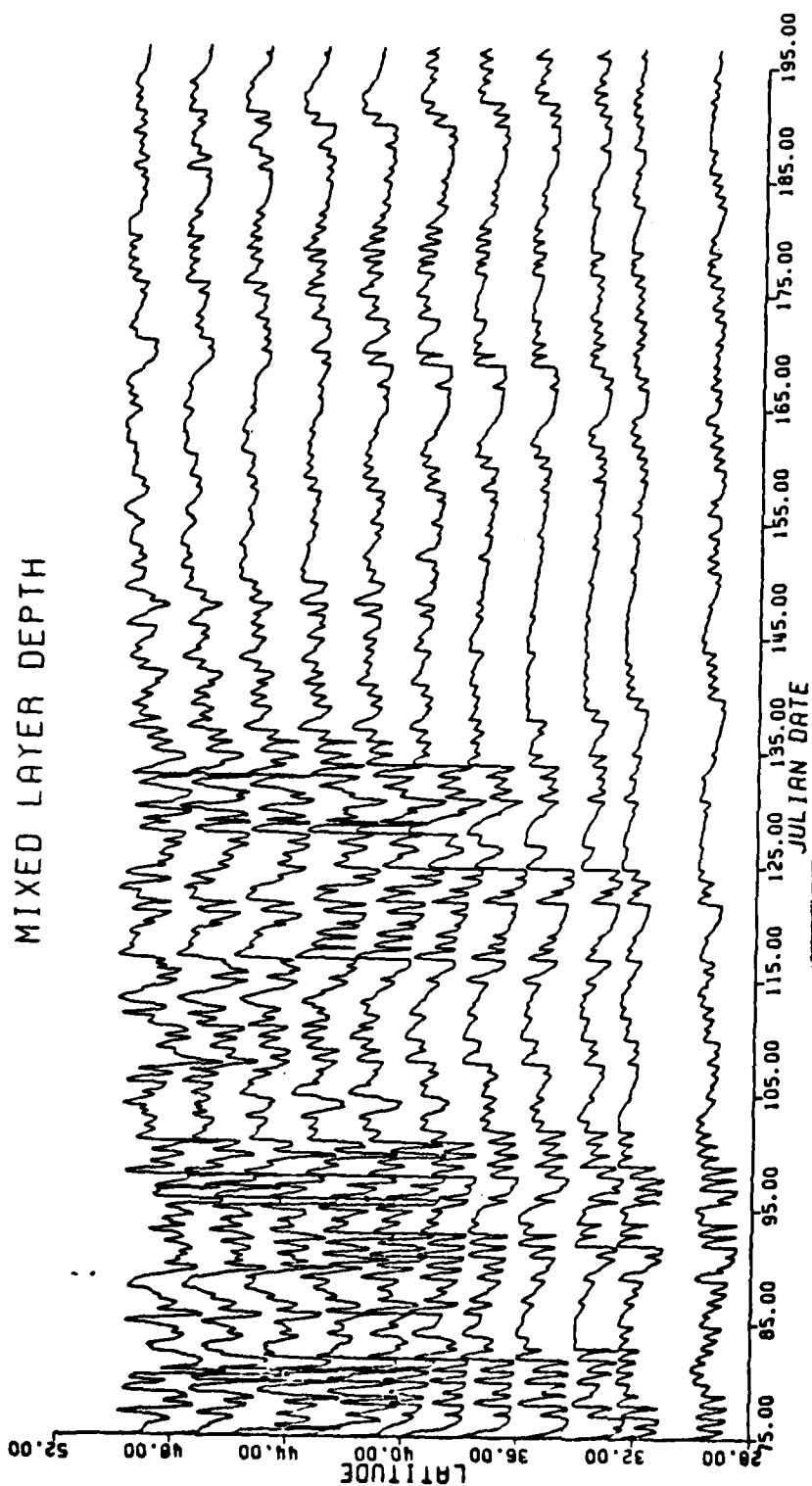


Fig. 9 Predicted mixed layer depth changes, relative to an initial depth ( 1 m) on 15 March 1976, at points along 155°W. Each 2° latitude corresponds to 100 m change in depth.



from the early part of the record to the later part. Large and rapid variations in layer depth were evident early in the spring, especially north of  $40^{\circ}\text{N}$ . This contrasted with the smaller and less frequent changes in depth during the late spring and early summer. Along  $155^{\circ}\text{W}$ , the transition period between the winter and summer mixed layer regimes occurred over a long period in the far north, whereas it seemed very rapid over the mid-latitudes, and was less distinct further south. The transition segment occurred earliest at southernmost latitudes, and was gradually later with increasing northerly latitudes.

A similarity between the traces was the time at which the deepening and shallowing occurred. There was greater variation of depth in the far north than in the south, but the time of the occurrences was nearly the same. Therefore, each of the latitudinal traces was similar to adjacent ones. This relationship became less valid late in the spring, when wind systems were less intense and affected smaller latitudinal bands.

The north-south range of concurrent shallowing and deepening events was greater during early spring, compared to similar events later in the season. This was a result of particular wind systems having more areal coverage early in the spring. For instance, on day 82, a rapid shallowing of the mixed layer depth was evident on all but the two southernmost traces. At  $34^{\circ}\text{N}$  and  $36^{\circ}\text{N}$ , the layer rapidly, but

temporarily, retreated to near the surface; whereas in the far north, the layer slowly retreated and remained relatively deep. Later in the record when the summer regime was fully established, a gradual deepening event from day 163 to 169 was only evident south of  $42^{\circ}\text{N}$ . An example of the mixed layer stability of the summer regime in mid-latitudes was evident during the same period. The layer steadily deepened for five days under the influence of moderately strong (15 m/s) winds, then rapidly retreated to near the surface. These same wind speeds occurred from day 129 to 134. The predicted trace for this period showed strong deepening the first two days and then significant diurnal fluctuations followed by a rapid retreat on day 134.

The corresponding mixed layer temperature traces for the 11 latitudes along  $155^{\circ}\text{W}$  are portrayed in Fig. 10. Due to the strong surface mixing, no significant temperature change was predicted over the northern part until late spring. Greater temperature response was revealed earlier in the record over the southern part. The diurnal temperature variation was more noticeable over the far south, but it became increasingly more apparent elsewhere towards late spring. The peak daily mixed layer temperature for any location was achieved three to six hours following the peak solar radiation flux.

Time series of mixed layer depths and temperatures along  $155^{\circ}\text{W}$  in 1977 showed a pattern similar to the previous

# MIXED LAYER TEMPERATURE

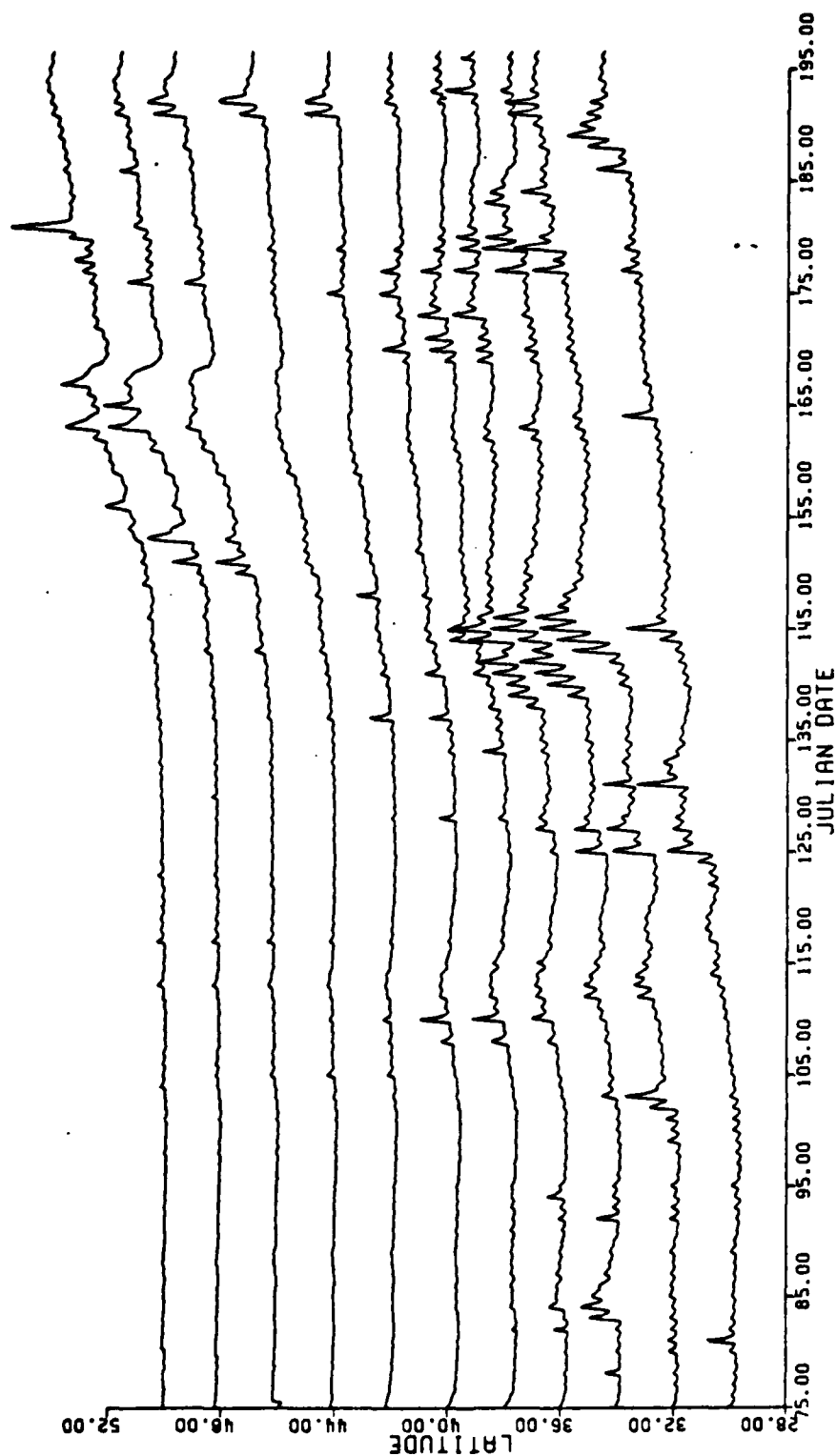


Fig. 10 Similar to Fig. 9, except for predicted mixed layer temperature changes. Each 2° latitude corresponds to 2C change in temperature.

year. The highly variable and relatively deep mixed layer did extend later into the spring, in response to more active winds over the north. The time series along 175°W, for both years, demonstrated more frequent shallow mixing depths over the south, with subsequently larger increases in temperature.

## B. TEMPERATURE PROFILES

The predicted temperature profiles of monthly mean values were drawn for March, April, May, and June of both years. Each profile was a 30-day mean computed at 10 m intervals from 0 to 190 m. An observed profile from the TRANSPAC analysis for June was plotted at depths 0, 30, 60, 90, 120, 150, and 200 meters. These profiles provided an illustration of the evolution of the mixed layer and the thermocline during the spring, as well as, verification of the accuracy of the predictions after 90 days.

In the vicinity of the permanent thermocline below 90 m, the agreement between the predicted and observed temperatures, was usually very good. From the June profiles of all locations, it was determined that the model temperature predictions, at the lowest depth of 190 m, were consistently colder than the 200 m observed temperature. This error is due to the lower boundary condition in the model. Above 90 m, there was considerable variation between the model prediction and the observations, especially prior to the corrections in the surface heat fluxes used by the model. From the original

model runs, all the June profiles at northern latitudes were up to 2.5 C too high at the surface and 30 m, whereas in southern latitudes, the predicted temperatures were sometimes greater than 5 C too low. At far southern latitudes, the predicted June profile was unrealistically cooler than the initial profile in March. In 1977 there were more locations, mostly in the northern latitudes, with better agreement of the profiles. This better agreement was probably related to the fact that the 1977 initial temperature profiles were cooler than in 1976.

The mean-monthly profiles for 38°N, 135°W in 1976 are shown in Fig. 11b. The March and April profiles were nearly isothermal above 100 m, while the May profile displayed warming in the upper 30 m. The June profile demonstrated close agreement with observed values. Fig. 11a contains the corresponding profiles for 38°N, 155°W in 1976. The first two profiles were nearly isothermal above 90 m, while the May profile indicated slight warming. In June, the predicted profile showed a significant change in the upper ocean, but the mean mixed layer temperature was 2.2 C cooler than the observed value of 17.5 C.

At both locations, nearly identical profiles were predicted in regard to the temperature and structure development. The weaker winds and earlier transition date at 38°N, 135°W, would seemingly have led to a warmer June temperature profile. However, the predicted profile was very close to the actual

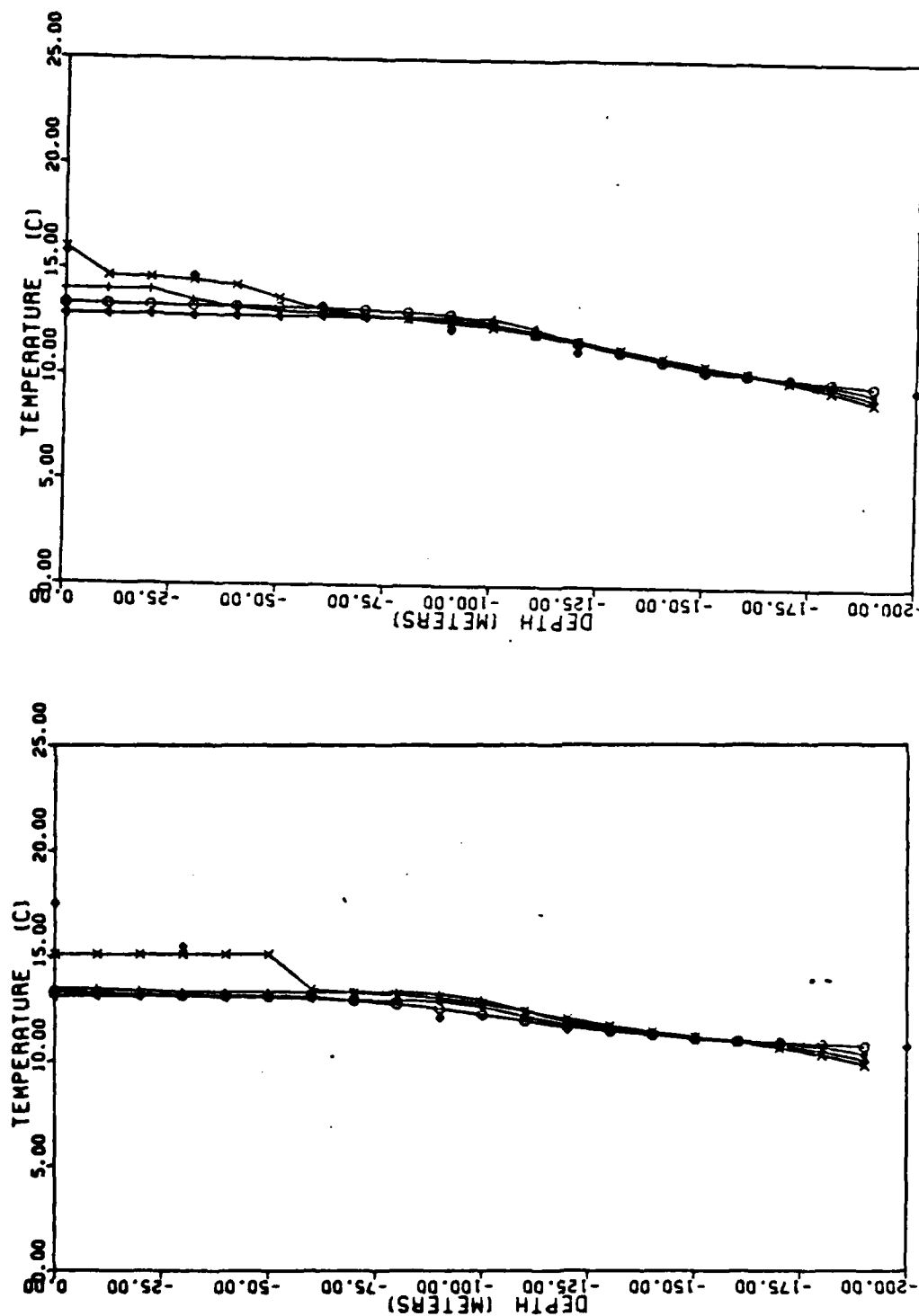


Fig. 11 Mean-monthly temperature profiles in 10 m intervals at 38°N, 155°W (left and 38°N, 135°W (right) for Spring 1976: March (circles), April (triangles), May (horizontal dashes), and June (diamonds). TRANSPAC analysis values for June (diamonds) for verification.

values, whereas at 38°N, 155°W, the model-produced, near-surface temperatures failed to match the verifying temperatures. The sea-surface temperature analyses of the North Pacific from the Fishing Information publications, by the National Marine Fisheries Service (NMFS), were used in conjunction with the TRANSPAC surface temperatures. The analyses were usually within 1 C. The NMFS analysis had better temperature resolution of the ocean polar and subtropical frontal zones. For June 1976, the 17.5 C surface temperature at 38°N, 155°W was about 1 C higher than normal, while the surface temperature at 38°N, 135°W was 15.7 C, and 0.5 C less than normal. It was therefore apparent that the anomalous warming at 38°N, 155°W, was not entirely produced by one-dimensional processes.

## V. CHARACTERISTICS OF TWO NORTHERN LOCATIONS

Two locations ( $46^{\circ}\text{N}$ ,  $175^{\circ}\text{W}$ ;  $46^{\circ}\text{N}$ ,  $155^{\circ}\text{W}$ ) were selected for comparison in 1976 and 1977 because they demonstrated behavior representative of the northern ocean. This set of points had the best agreement between the cumulative heat flux and observed heat content for the original calculations.

The wind at  $46^{\circ}\text{N}$ ,  $155^{\circ}\text{W}$  in 1976 (Fig. 12) was quite strong until the layer transition on day 150--after which the speed remained below 5 m/s for three days. A ten-day period of continuous downward heat flux and minimum solar flux ensued. The transition was a gradual, multi-step process from 18 GMT on day 147 to 00 GMT on day 150. During the transition, a rapid rise in mixed layer temperature from 7.8 C at 15 GMT on day 149 to 9.8 C at 03 GMT on day 151 took place. A sharp wind increase on day 169 brought a significant temperature reduction.

At  $46^{\circ}\text{N}$ ,  $175^{\circ}\text{W}$  in 1976 (not shown), the wind speed was slightly higher and more variable than at  $46^{\circ}\text{N}$ ,  $155^{\circ}\text{W}$ . The mixed layer at both locations, remained quite deep through the spring. A sharp transition, from 18 GMT on day 144 to 00 GMT on day 145, occurred during a lull in the wind. A high wind event around day 179 produced steady deepening of the mixed layer. Even though the summer thermocline had formed, considerable variability in mixed layer depth was evident following the episode.



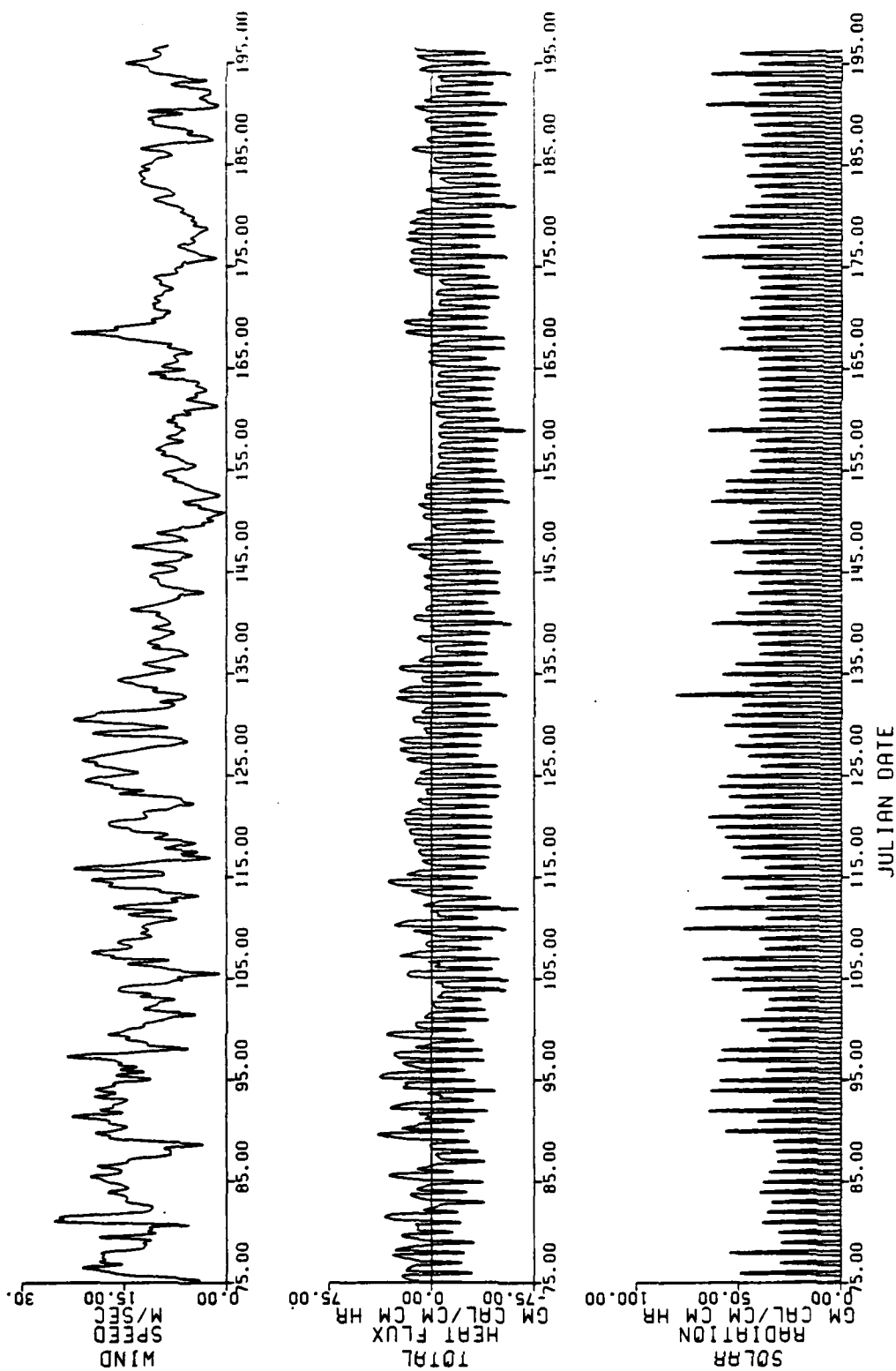


Fig. 12 Similar to Fig. 6, except at 46°N, 155°W in 1976.

In 1977, the latest transition period of all locations was at 46°N, 155°W, with a two-step process from 18 GMT on day 161 to 00 GMT on day 163. Prolonged high wind speeds and extensive cloudiness (implied by small solar flux values) are depicted in Fig. 13. These conditions allowed the relatively deep and variable mixed layer to persist through most of the spring. At 46°N, 175°W a sharp transition from 18 GMT on day 140 to 00 GMT on day 141 produced a temperature increase of 1 C to 6.4 C at 06 GMT on day 141. Strong winds prior to the transition were much diminished afterwards, and this is reflected in the change in character of the mixed layer depth trace. One of the largest temperature increases, 2.5 C in 12 hours, occurred at this location during a period of nearly calm winds.

The predicted mean-monthly temperature profiles for 46°N, 175°W during 1977 are shown in Fig. 14a. The March profile was coldest at 30 m and became warmer with increasing depth. April and May profiles were isothermal, while the upper portion of the June profile warmed sufficiently to nearly match the observed values. The 1977 profiles for 46°N, 155°W in Fig. 14b were nearly identical in structure, except the predicted near-surface temperatures during June were about 1 C less than the TRANSPAC temperatures. At both locations, the March profiles became cooler from the surface to 30 m, and then warmer with depth. This excessive cooling of the upper ocean is characteristic of the far northern latitudes in winter

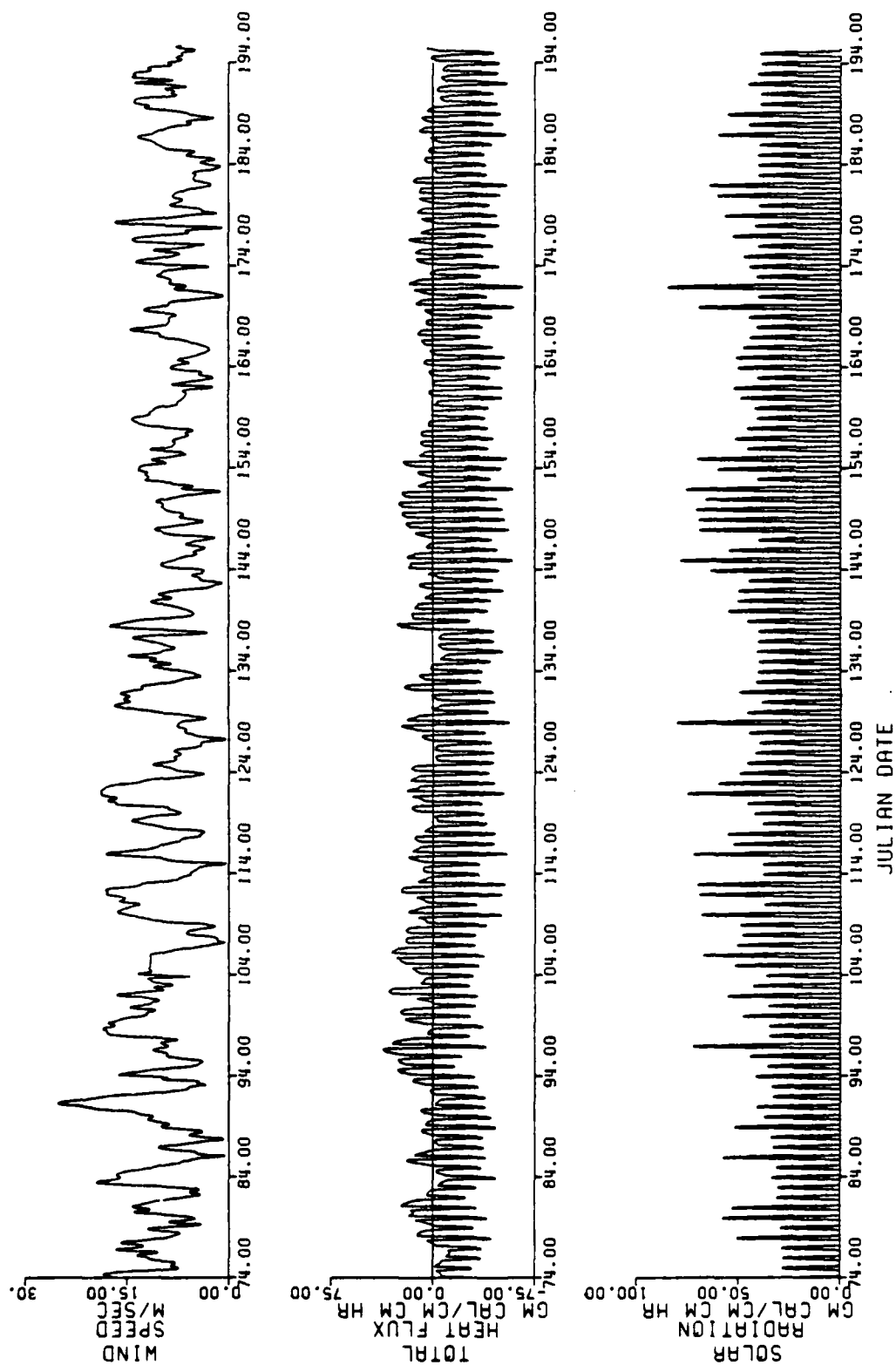


Fig. 13 Similar to Fig. 6, except at 46°N, 155°W in 1977.

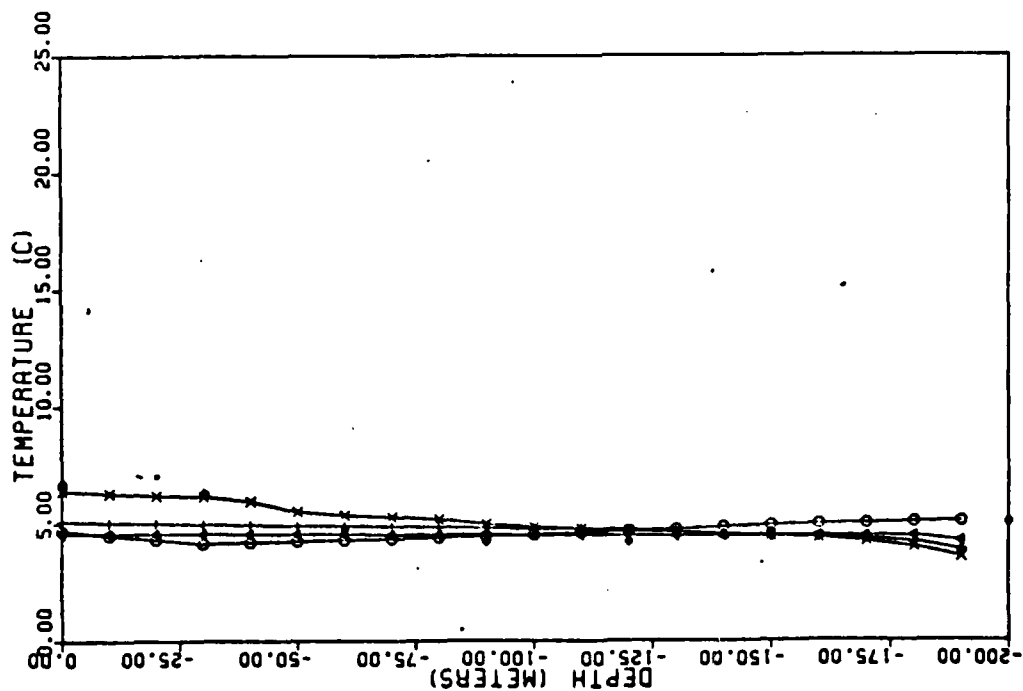
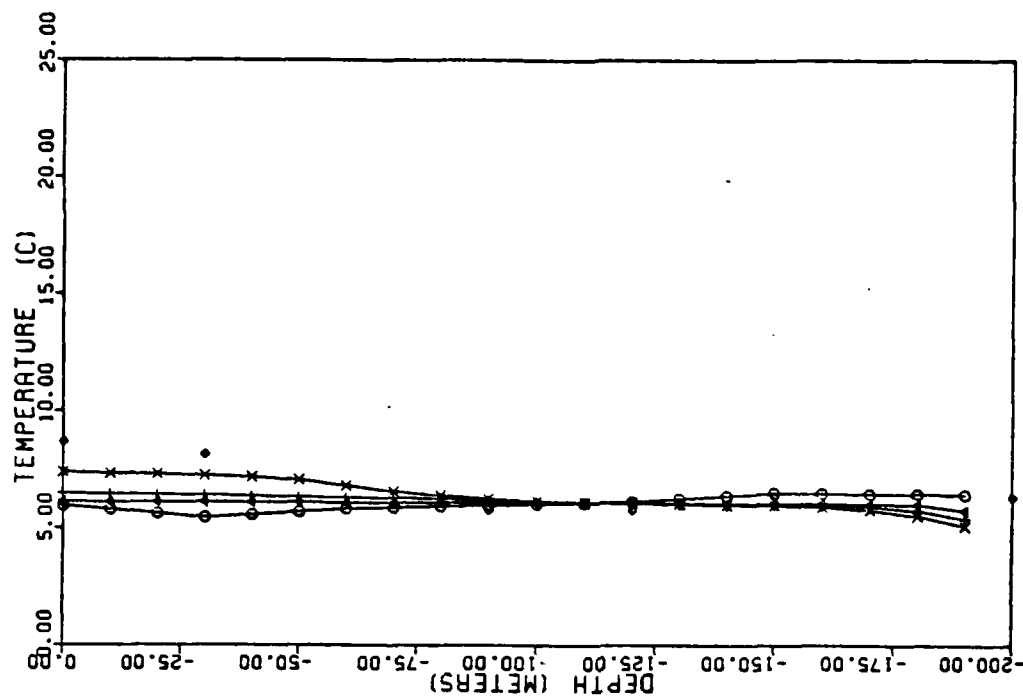


Fig. 14 Similar to Fig. 11, except at 46°N, 175°W (left and 46°N, 155°W (right) for Spring 1977.

and early spring, because of the frequent periods of cold, continental air passing over these waters.

Verification of the mean-monthly sea-surface, or mixed layer temperatures, between the model predictions, the TRANSPAC observations, and the NMFS analysis were compiled in Table 1. The last row contained the estimated departure of the NMFS temperature from the 20-year mean. These values confirmed that the upper ocean during the spring was considerably cooler than normal at the two points in both years, although in June the departures were insignificant.

TABLE 1.

Mean-monthly sea-surface temperatures (C) from model predictions, TRANSPAC observations, NMFS analysis, and the estimated departure from normal, at two locations in 1976 and 1977.

1976	46°N 175°W				46°N 155°W			
	MAR	APR	MAY	JUN	MAR	APR	MAY	JUN
Model	5.0	5.0	5.7	7.5	6.3	6.5	7.0	8.9
TRANSPAC	5.0	4.5	4.9	6.5	6.3	5.8	6.6	9.4
NMFS	5.5	5.3	5.7	7.5	6.4	6.2	6.9	9.0
Est. Dept.	0.0	-1.1	-0.8	0.1	-0.6	-1.3	-1.2	-0.4

1977	46°N 175°W				46°N 155°W			
	MAR	APR	MAY	JUN	MAR	APR	MAY	JUN
Model	4.7	4.7	5.2	6.4	5.9	6.1	6.7	7.5
TRANSPAC	4.7	4.0	5.2	6.7	6.0	6.6	6.9	8.7
NMFS	4.8	4.5	5.2	7.5	6.0	6.8	7.8	9.6
Est. Dep.	-0.7	-1.9	-1.3	-0.1	-1.0	-0.7	-0.3	+0.2

Taking into account the sparse ocean data available for analyses, 0.5 C is about the best accuracy that can be achieved in comparing the predictions and two sets of observations. Unfortunately, this error is of the same order as a majority of the analyzed anomalies. In 1976, very good agreement was

noted between the mean-monthly temperatures predicted by the model and the NMFS analyses, especially in June. In 1977, the more favorable comparison with the model prediction was the TRANSPAC observation. At  $46^{\circ}\text{N}$ ,  $155^{\circ}\text{W}$ , however, the June model prediction was substantially less than the observations. Aside from that discrepancy, it was evident that at these locations, the mixed layer temperature evolution was mainly a one-dimensional process.

## VI. ADJUSTED HEAT FLUX AT 30°N, 175°W IN 1977

Adjustments in the FNOC total heat flux calculations were made in an initial attempt to rectify the problem of excessive upward heat flux in the southernmost latitudes. The interpolated total heat flux values for 30°N, 175°W in 1977 was reduced by  $10 \text{ cal cm}^{-2} \text{ hr}^{-1}$ . This reduction value was nearly the same as the correction field value for that location as shown in Fig. 4b. Model predictions were compared for the adjusted and the original upward heat fluxes using the same wind speed and solar radiation flux.

The unadjusted mean-monthly temperature profiles at 30°N, 175°W (Fig. 15a) show coincident April, May, and June profiles with lower temperatures than the initial March profile. The observed June temperatures above 90 m were much higher than all of the predicted profiles. The  $10 \text{ cal cm}^{-2} \text{ hr}^{-1}$  adjustment, as shown in Fig. 15b, produced profiles with a more realistic configuration. The predicted mean surface temperature in June was nearly the same as the observed temperature, while the remainder of the profile approached the observations. The base of the mixed layer appeared to have been between 10 and 20 meters.

The change in the response of the mixed layer to the corrections of surface heat flux is displayed in Fig. 16. Each 2° of latitude corresponds to a 100 m change in depth.

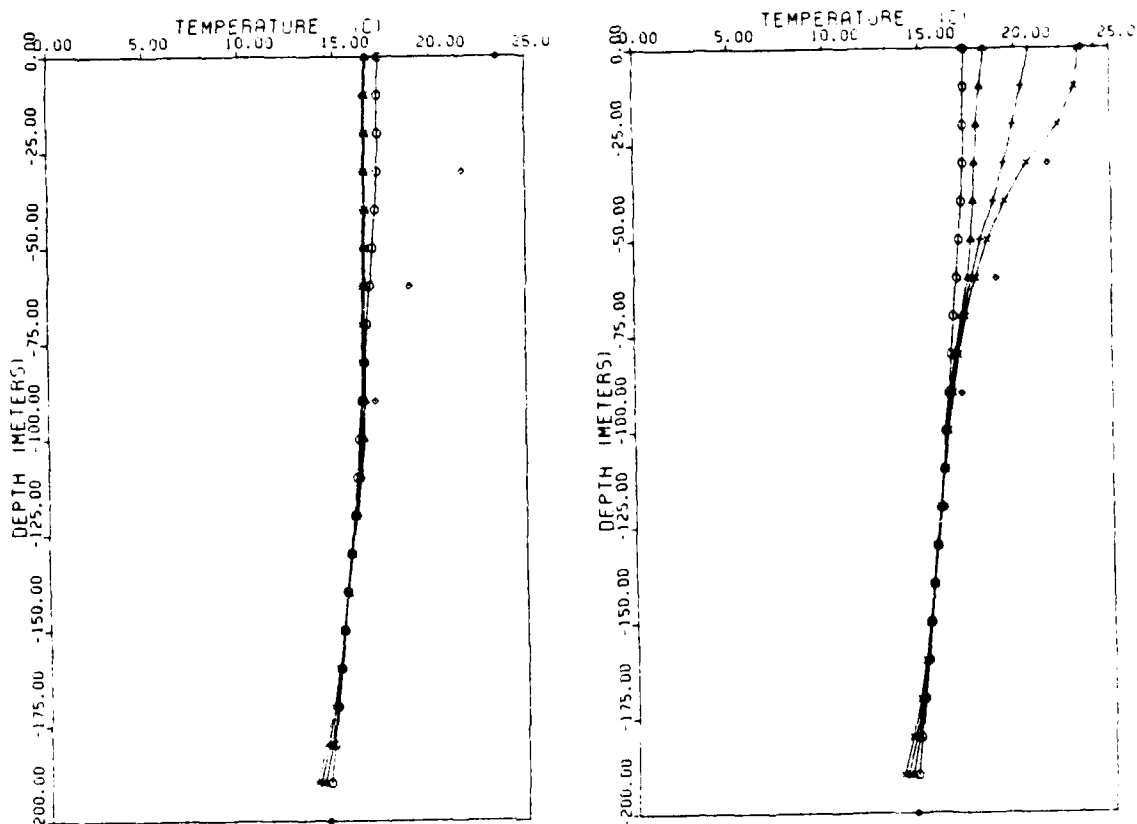


Fig. 15 Similar to Fig. 11, except for Spring 1977 at 38°N, 175°W with unmodified values (left) and reduction of heat flux by 10 cal cm<sup>-2</sup>hr<sup>-1</sup> (right).



# 175°W MIXED LAYER DEPTH 1977

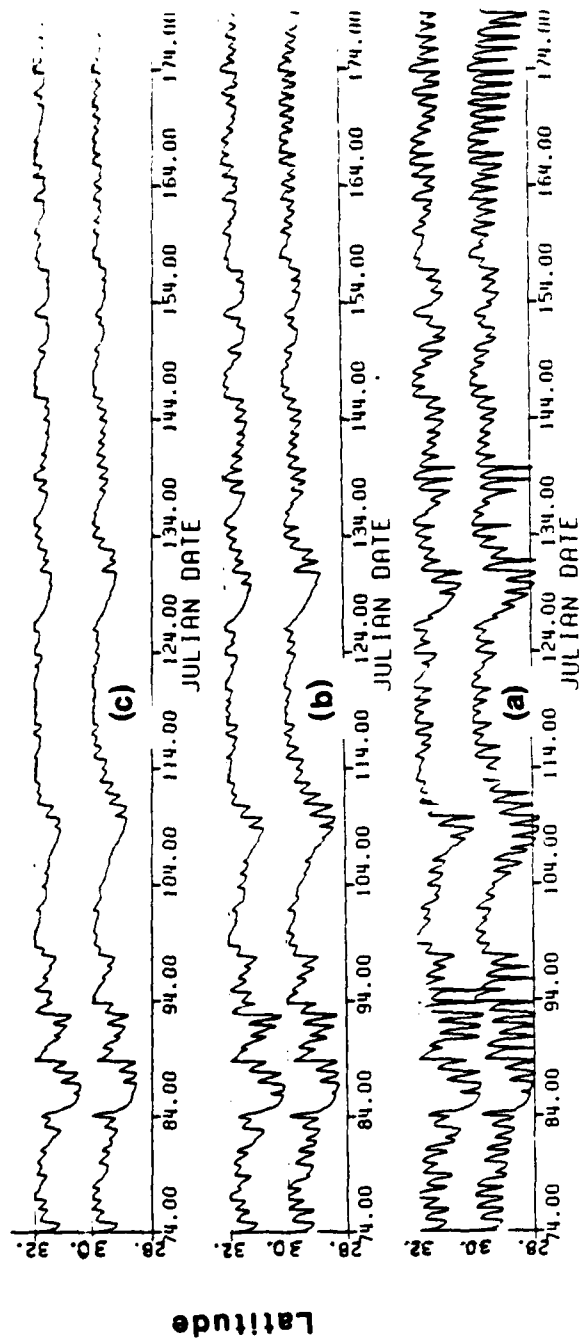


Fig. 16 Predicted mixed layer depth changes at 30°N and 32°N along 175°W for (a) unmodified values, (b) 5 cal cm<sup>-2</sup> hr<sup>-1</sup>, and (c) 10 cal cm<sup>-2</sup> hr<sup>-1</sup> reduction of heat flux. 2° latitude corresponds to a 100 m change in depth.

The greater differences were in late spring and early summer. During this period, the predicted layer depths using the unadjusted heat fluxes displayed large diurnal variability, while the record with the  $10 \text{ cal cm}^{-2} \text{ hr}^{-1}$  reduction exhibited a shallow and stable mixed layer. Early in the spring, the character of the predicted mixed layer depth traces was similar, but the model run with the larger adjustment did not have the unrealistic diurnal signal during summer.

The displayed results demonstrated that it was feasible to reduce the disagreement between observed and predicted values by correcting the total heat flux field. Similar changes in the heat flux field were used in adjusting the cumulative heat flux to conform with the observed heat content, as described in section II.

## VII. SPRING TRANSITION

### A. DEFINITION

To determine quantitatively when the ocean boundary layer changed from a winter to a summer regime, a set of criteria was formulated based on the predicted mixed layer depths. This evaluation technique was applied to the locations within the ADS area shown in Fig. 1, and produced a representative spatial distribution of transition dates.

The time series plots of mixed layer depths, as well as 3-hourly print-outs, were used to determine manually the spring transition dates. The transition date was defined as the first period of sustained shallow mixed layer depths ( $\leq 20$  m) that followed a period of greater than 60 m depths. Near the northern boundary, the predicted depths may have later exceeded 60 m for a short period a week or more after the establishment of the stable layer. Consequently, the transition date was specified, as that period that coincided with a significant increase in mixed layer temperature. The transitions at all locations generally coincided with a mixed layer temperature increase that signalled the formation of the seasonal thermocline.

Another quantitative method that could have been used in selecting a transition date was the determination of the starting time of a prolonged increase in mixed layer temperature.

This type of temperature increase would have only been realized if the mixed layer remained shallow for several days. The drawback of this method was that the selection of the transition date would have been based on a change in temperature, which was the effect being evaluated, and not on the change in depth, which was the cause being investigated.

#### B. DESCRIPTION

Prior to the heat flux adjustments, the mixed layer depth predictions near the southern boundary were unrealistic, and transition dates were difficult to determine. This problem was solved after the corrections to the cumulative heat fluxes were made.

The spring transition dates for all sampled locations in the ADS region were plotted for each year in Fig. 17. In 1976, the earliest dates were in the northern part along  $155^{\circ}\text{W}$ . The first transition date was day 79 (March 19) at  $32^{\circ}\text{N}$ ,  $165^{\circ}\text{W}$  and  $30^{\circ}\text{N}$ ,  $175^{\circ}\text{W}$ . The last date was day 153 (June 1) at  $50^{\circ}\text{N}$ ,  $155^{\circ}\text{W}$ . The transition dates were sometimes recorded in latitudinal bands, or small groups extending northward two to five degrees latitude. In some cases the latitudinal extent of an apparent transition was much greater, but a subsequent storm would again deepen the layer in the poleward regions. Surprisingly, the longitudinal variation in dates was as large as the latitudinal variation over the middle and southern portion.

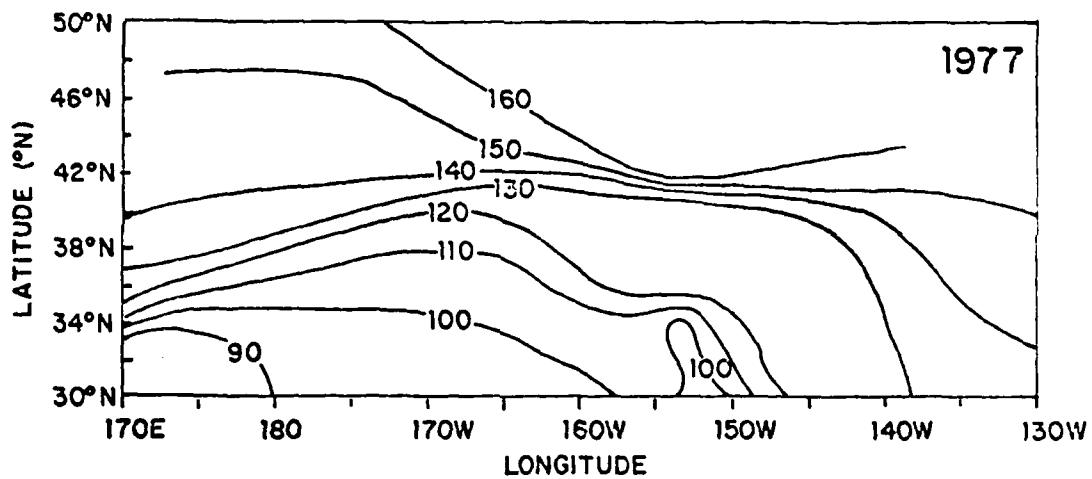
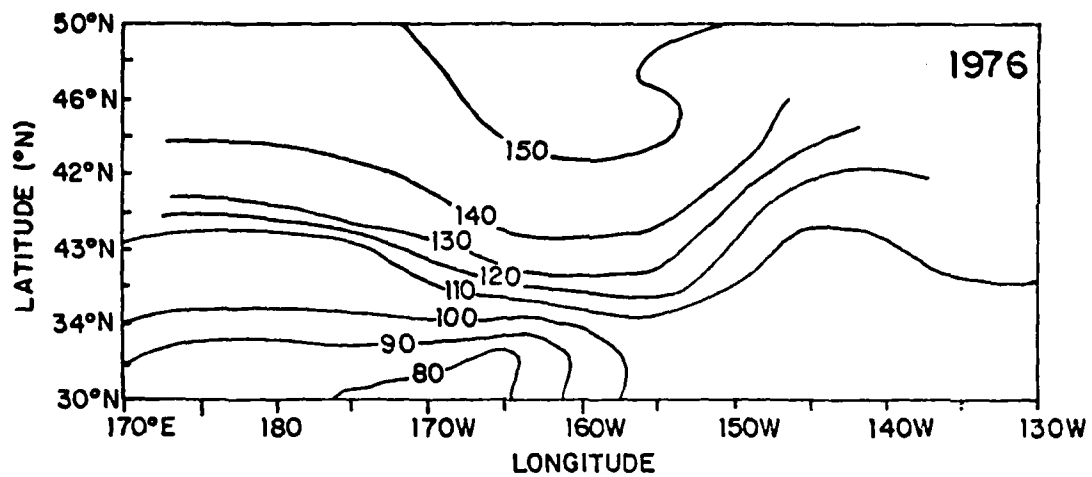


Fig. 17 Spring transition dates (Julian) for the sampled locations within the ADS area for 1976 and 1977.

In 1977, there was a similar temporal pattern to that of 1976, although the transition occurred considerably later. The mean date of the 1976 sample was day 121 (April 30), while the mean date in 1977 was day 127 or May 7. The earliest transition date was day 86 (March 27) at 32°N, 175°E, while the latest date was shared by 42°N, 44°N, and 46°N along 155°W on day 163 (June 12). A 33-day change in transition date over the year occurred at 38°N, 135°W.

### C. COMPOSITING

To present the common features of a spring transition, the forcing fields and predictions of mixed layer depth and temperature, were composited with respect to the transition date. Since all of the parameters had a strong diurnal component, the transition was expected to be near 00 GMT for each location. Note that 00 GMT corresponded to local noon at 175°W and 1500 local at 135°W. Hourly adjustments had to be made at locations east of 175°W, so that the transitions occurred at the same time of day.

Compositing was done for the six points along 38°N and 32°N, and for eleven points along 155°W and 175°W, for both years. A representative sample of 10 days prior and 20 days after the transition was chosen as sufficient time in which to investigate the parameters. This period of time spanned about eight to ten synoptic periods. The set of transition dates derived from the unadjusted heat flux model runs was used for the compositing technique.

The composite along  $38^{\circ}\text{N}$  in 1976 revealed the most distinctive features relative to the transition time, because it contained the least number of locations with heat budget disagreements. Although the composites along  $175^{\circ}\text{W}$  and  $155^{\circ}\text{W}$  contained more points, they included the troublesome southernmost latitudes, where transition dates were in doubt. That uncertainty detracted from the composited traits of an actual transition. In Fig. 18, day 0 on the abscissa was the transition time, with an interval 10 days prior to transition plotted to the left, and a 20-day interval after transition to the right.

The mixed layer depth composite in Fig. 18a exhibited considerable variation, with a large mean depth preceding the transition, and little variation about a shallow depth following the transition. This composite was not independent of the transition date, because the date was chosen from criteria based on these characteristics. The mixed layer temperature composite showed the deviation of temperature with respect to the mean temperature of the 30-day record. Preceding the transition day, the temperature was less than the mean, and showed almost no variation. The first notable increase coincided with the mixed layer transition. Thereafter, the temperature steadily increased and became more responsive to diurnal variations.

The behavior of the composited forcing functions (Fig. 18b) was independent of the transition date selection process. The wind speed composite revealed that there was a sharp drop

Fig. 18b

Composite of atmospheric forcing parameters for 6 locations along 38°N in 1976, relative to the transition dates (day 0).

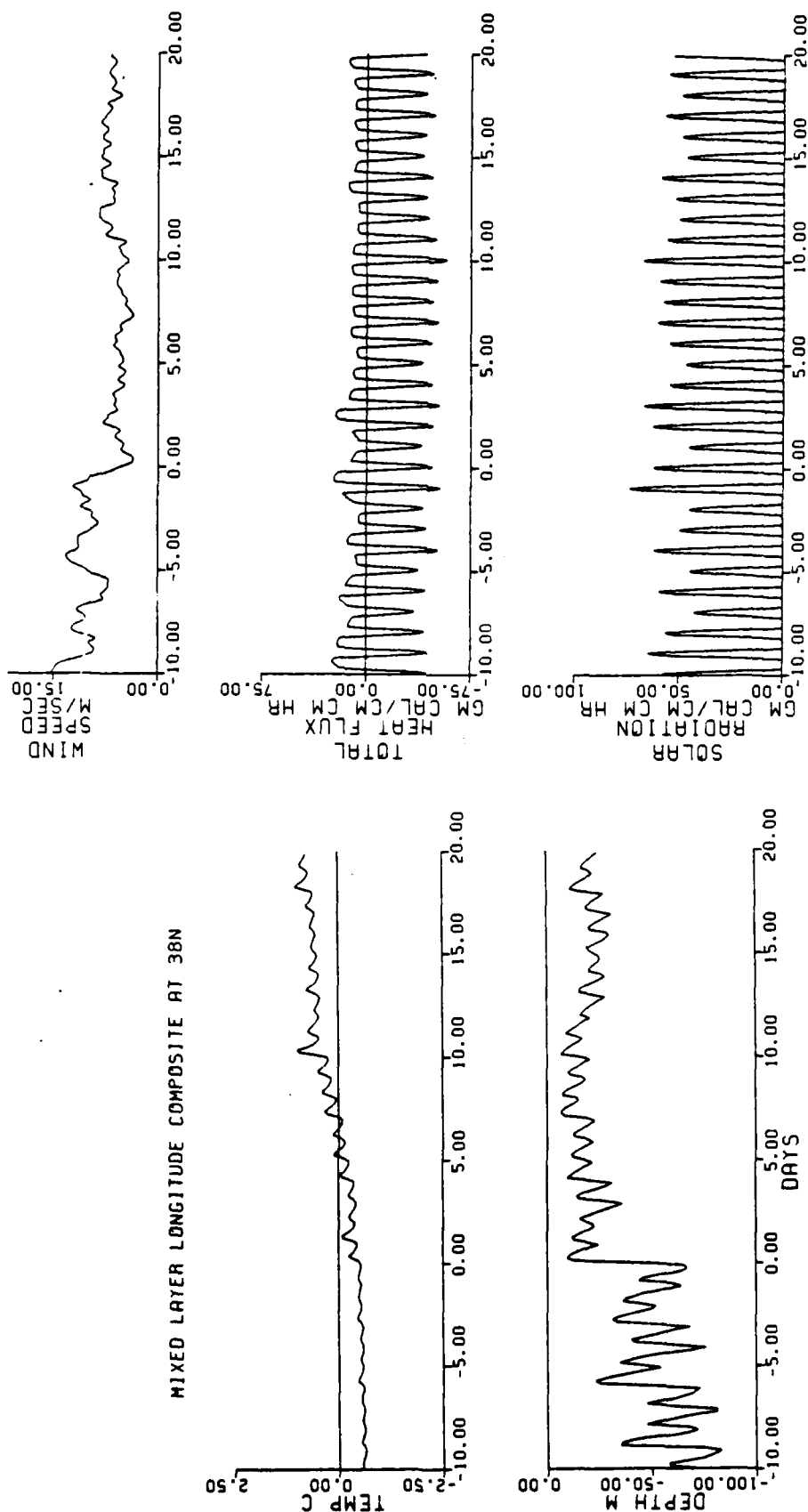


Fig. 18a Composite of model-predicted mixed layer temperature (upper) and depth (lower), for 6 locations along 38°N in 1976, relative to the transition dates (day 0). Upper composite displays the deviation of temperature (C), with respect to the mean temperature of the 30-day record.



in wind speed during transition. This was the most distinctive atmospheric forcing feature associated with the transition. The wind speeds prior to the transition were higher, and showed a greater variation, than the weaker and steadier winds afterwards. The wind speed of 5.7 m/s, at day and time zero, was a drop of over 6 m/s from a peak speed of 12.2 m/s, which occurred 23 hours earlier. The lowest speed of 3.6 m/s was reached ten hours later, during the night. The subsequent rise to the next peak wind speed of 7.8 m/s took place 42 hours after the transition. For all locations in both years, the mean wind speed at transition time was 4.5 m/s.

The total heat flux composite showed that there was a large upward flux during the night preceding the transition, and an average heat loss during the following two nights. More daily variation was evident before the transition than afterwards. This heat flux pattern was consistent with the behavior of the wind speed variations. The solar flux composite did not exhibit any significant changes throughout the 30-day record, although there was a relatively high value on the day before, and a low value on the day after the transition. The time changes in fluxes of solar radiation and total heat were apparently of much lesser importance than were the wind speed variations in bringing about the change of the mixed layer from a winter to a summer regime.

#### D. STATISTICAL VALIDATION

How reliable was the method of using the changes in mixed layer depth for selecting the transition date? If the method is valid, there should have been a statistically different regime before the transition than the regime following transition. According to the information provided by the composites, the wind speeds should also have been statistically different before and after the transition.

The method selected for evaluating the different groups was the "t-test" for two independent samples. This procedure determines if the means of two collections are different at a given level of significance. Dividing the difference between the two means by the standard error of the difference yielded a statistic

$$t = (M_1 - M_2) / (S_{m_1 - m_2})$$

which was distributed as the t-distribution, if the two population means were equal. To the extent that the two means were not equal, the expected value of the calculated "t" would have been inflated, and the probability of rejecting the null hypothesis (of equal means) would have become greater than the level of significance. The assumptions underlying this estimate were that the data in both samples were normally distributed, and the variances of the two populations were equal. Moderate departures from these assumptions have proved to be of no practical consequence. When the two samples were

of nearly equal size, the statistical test was quite insensitive to violations of these assumptions. The standard error of the difference was just the standard deviation, and was computed according to

$$S_{m_1-m_2} = (\theta_1^2/n_1 + \theta_2^2/n_2)^{1/2}$$

where  $\theta_1^2$  and  $\theta_2^2$  were the variances of the two groups, and  $n_1$  and  $n_2$  were the respective number of observations (e.g. Roscoe, 1969).

The composites of wind speed and heat flux contained hourly interpolated values, of which only a fraction were independent observations. The 12-hour observations were considered as independent of each other, so that the 60 values for the 30-day record, allowed 58 degrees of freedom. The mixed layer depth predictions composite was treated similarly.

TABLE 2.

Determination of statistically different means of mixed layer depth, wind speed, and heat flux, prior to and after the transition day, from the composite along 38°N in 1976. The first two columns contain the means before and after the transition. The standard deviation in the third column is followed by the resultant "t-value" in the next column. The threshold "t-value" for 58 degrees of freedom, at a .05 level of significance for a two-tailed test is 2.0.

	$M_1$	$M_2$	$S_{m_1-m_2}$	t
Mixed layer depth	54.44	18.46	3.43	10.49
Wind speed	10.45	6.19	0.47	9.06
Heat flux	-3.34	-8.32	6.07	0.82

The two means of the mixed layer depth and wind speed were shown to have been significantly different, while the two means of the heat flux were not significantly different. The outcome of this test was repeated using the other composited latitudes and longitudes. The general inference of the results was more important than the computed values, because the variances of the two samples were not equal. Fortunately, the "t-test" was much more sensitive to the assumption of equal means (null hypothesis), than to the assumptions of normality or homogeneous variances. Nonetheless, the transition date was the appropriate division between the two samplings of the mixed layer depth and wind speed, but it had no significance in the heat flux record. Thus, the method for selecting the spring transition date employed in this study proved adequate.

### VIII. SYNOPTIC DESCRIPTION SURROUNDING SPRING TRANSITIONS

The mixed layer spring transition often occurred during a period of weak winds. An atmospheric high pressure area usually provided two or three days of favorable conditions for light winds. It was not surprising then that the location was found close to the center of a high pressure area on the date of a transition. In a few instances the transition location was near the center of a well-developed low pressure system. The sea-level pressure at the time of transition was mostly above 1020 millibars (mb), and occasionally in excess of 1030 mb.

#### A. 1976 (MARCH-JULY)

The group of transition dates over the southwestern ADS area occurred earlier than over the remainder of the domain, because of the presence of a high pressure area. During March, a large high pressure cell, with sea-level pressures up to 5 mb above normal, was centered near 35°N, 135°W, and covered most of the eastern North Pacific south of 45°N. The earliest transition dates were not found near the center of this high pressure area, because steady winds continuously mixed the upper ocean layer. Meanwhile, sea-level pressures were up to 5 mb below normal over the Aleutians and the Gulf of Alaska. This increased pressure gradient maintained strong

west to northwest winds between  $40^{\circ}\text{N}$  and  $55^{\circ}\text{N}$ , which contributed to the production of below normal sea-surface temperature anomalies. The mean pressure pattern of March lasted well into May, even though the southern high pressure area built westward, and the Gulf of Alaska low pressure area deepened.

During mid-April transitions took place at the remainder of the locations south of  $40^{\circ}\text{N}$  except in the central portion, where strong mixing postponed the change. It was not until mid-May though, that the transitions materialized in the mid-latitude, ocean polar front region. Thereafter, a series of high pressure systems over the north portion allowed transitions to occur through the end of May. At the northernmost locations the spring transitions tended to occur under weak pressure patterns, rather than under a well-defined high pressure area, as was the case with the majority of the transitions.

In June, the subtropical anticyclone was positioned near  $37^{\circ}\text{N}$ ,  $145^{\circ}\text{W}$ , with up to 5 mb above normal pressures over the entire eastern North Pacific. Large sea-surface temperature increases over the east-central ADS area between  $150^{\circ}\text{W}$  and  $170^{\circ}\text{W}$  may have been aided by warm water advection. The model-produced, mixed layer temperatures did not predict this anomalous development. During July, the strong high pressure cell collapsed as above normal westerly winds developed between  $35^{\circ}\text{N}$  and  $45^{\circ}\text{N}$ , and the warm anomaly region of the previous month dissipated [National Marine Fisheries Service, 1976].

B. 1977 (MARCH-JULY)

The atmospheric circulation patterns returned toward normal positions in March, after five months of unusually low pressures and persistent high winds in the central and western North Pacific. As the Aleutian Low shifted eastward toward the Gulf of Alaska, the eastern Pacific High, which had remained nearly stationary during the winter along the North American west coast, moved southwestward toward its normal position near  $35^{\circ}\text{N}$ ,  $145^{\circ}\text{W}$ . Although surface pressures north of  $45^{\circ}\text{N}$  returned to near normal in March, the strong high maintained the pressure gradient, which allowed the continuation of higher winds and strong ocean mixing west of  $150^{\circ}\text{W}$ . In April, the high moved westward to near  $33^{\circ}\text{N}$ ,  $175^{\circ}\text{W}$  and became less dominant. The general circulation in the North Pacific was considerably weaker, except for the area west of  $155^{\circ}\text{W}$  from  $37^{\circ}\text{N}$  to  $47^{\circ}\text{N}$  [National Marine Fisheries Service, 1977].

The first transitions of the season took place in the southwestern portion of the ADS region, under a high pressure event at the end of March and the first part of April. Following a prolonged period of high pressure from late April to early May over the southern ADS area, the remainder of the transitions occurred south of the ocean polar front. The mean atmospheric circulation in May was close to the average, as the subtropical high returned to a position near  $33^{\circ}\text{N}$ ,

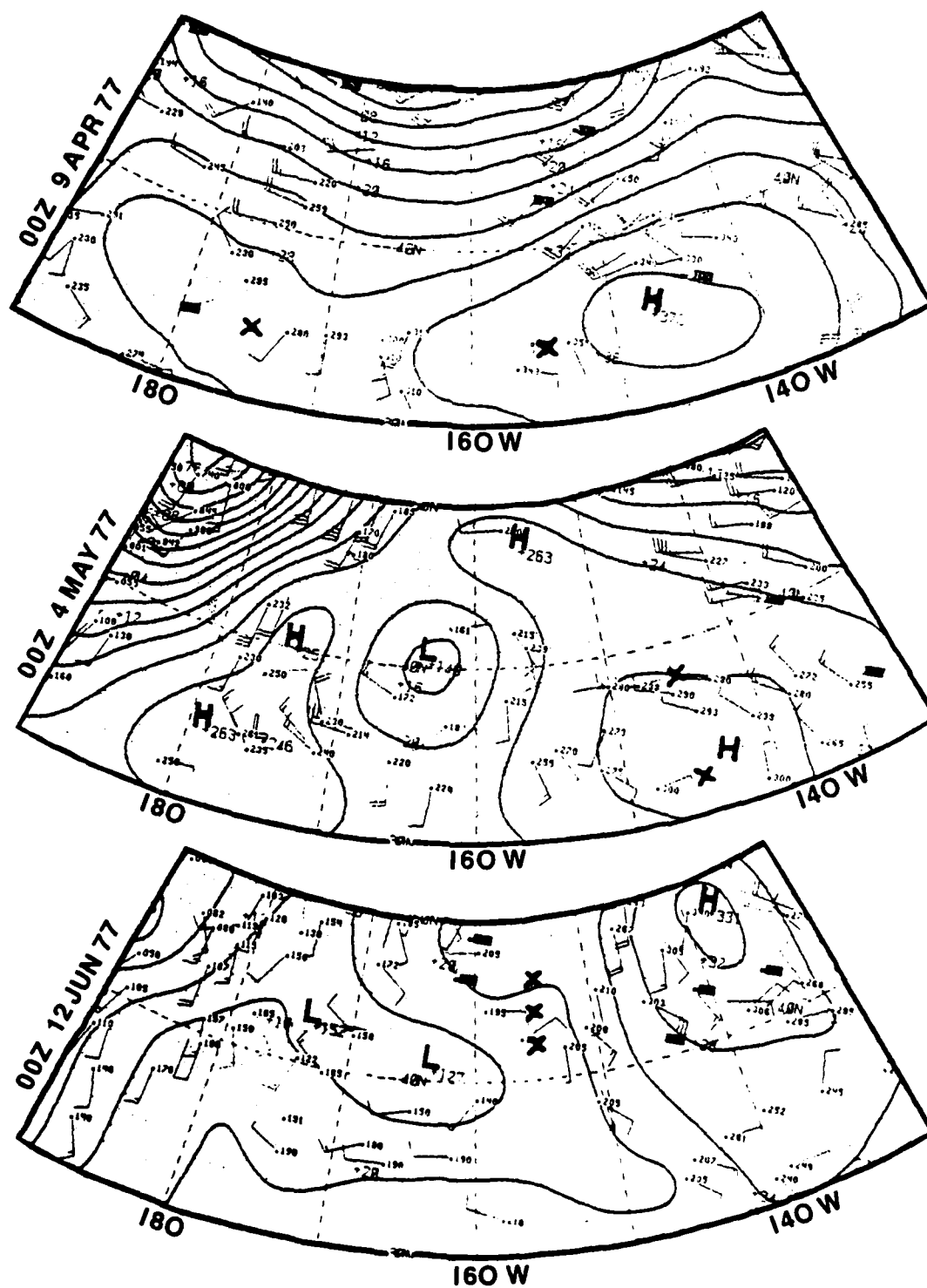
150°W. Towards the end of the month, the weakened pressure pattern over the northeastern ADS area permitted transitions in this section. Persistent high winds delayed the transitions along 155°W until mid-June.

In June and July, the observed mean pressure pattern was similar to the normal. The weak subtropical high was situated between 145°W and 155°W along 35°N. As a result of two successive months of near normal atmospheric circulation, most of the sea-surface temperature departures from normal were less than 1 C in the eastern North Pacific. However, temperatures remained significantly below normal over large areas in the central Pacific, as they had been since the winter.

Atmospheric surface pressure patterns within the ADS area were chosen for selected transition dates in 1977. These map sections (Fig. 19) were reproduced from the FNOC North Pacific sea-level pressure analyses. They presented typical synoptic situations with respect to transition locations (marked by X's) for early spring, mid-season, and late spring.



Fig. 19 Sea-level pressure patterns within the ADS area reproduced from the FNOC North Pacific analyses. Transition locations (marked by X's) Julian days 99, 124, and 163 in 1977.



## IX. SEA-SURFACE TEMPERATURE ANOMALY GENERATION

An earlier than normal mixed layer transition was expected to have been related to the development of higher than normal sea-surface temperatures. This relationship held rather well for the 19-year sample at OWS "P" (50°N, 145°W) [Elsberry and Garwood, 1978]. At this location, the median transition date was day 117 (April 27), with a range of about 70 days, and most of the values occurred between days 100 (April 10) and 140 (May 20). The 1976 and 1977 transition dates from the present model and forcing appeared to have been equal or greater than day 140 for the region near OWS "P". These values compare unfavorably with the median transition date for OWS "P" from the Elsberry and Garwood (1978) study. This may be indicative of the anomalous oceanic conditions during 1976 and 1977, or that the atmospheric forcing used in this study may have been inadequate.

Determining the deviation of the spring transition data from the long-term mean, as was employed at OWS "P", was not applicable to this study, since there were only two years involved. The spring transition occurred much later in the northern part of the ADS area than in the south, so just comparing the transition dates to the SST anomalies would have given an unrealistic relationship. However, if a transition

date occurred earlier in one year than in another for a given location, then there should have been a greater SST anomaly development during the earlier year.

#### A. OBSERVED ANOMALIES

The observed surface temperature anomalies drawn by the NMFS were the deviation of the mean-monthly SST from a 20-year (1948-1967) normal. Within the ADS area in March 1976, the southeastern portion was much warmer (1-1.5 C) than the rest of the area. In April, the center of the warm anomaly shifted ten degrees of longitude to the west and weakened. During May, this area translated five degrees farther southwestward, while cold anomalies proliferated in the northern part. Strong warming of the central portion was registered in June, but the anomaly disappeared in July. In March and April 1977, the SST of the central portion was well-below normal (1.5-2.5 C), while in the far eastern side, it was slightly above. For the next three months, cold anomalies remained over the central portion, in spite of some warming during May.

#### B. EVALUATION METHODS

For both years, the March anomalies were subtracted from the July anomalies at each location. With the initial conditions removed, only the anomalies generated over the 4-month period were evaluated. The difference in the transition dates between 1976 and 1977 at each location was plotted as a function

of the difference in the adjusted SST anomalies. It was expected that a large positive transition date difference would directly correspond to a large, positive anomaly. That is, the earlier the transition date, the higher the temperature anomaly would have been. Only about one half of plotted points conformed with this reasoning. The 3-month net change in SST from March to June was also computed for both years, and the difference was compared to the difference in transition dates. Once again, the results were inconclusive.

There were a couple of reasons why little, if any, correlation of the results was shown. The accuracy limit of the analyses and predictions was around 1 C, while the actual SST anomalies were often only plus or minus 1 C. Therefore, the errors and investigated values were of the same magnitude. In the central North Pacific, the anomalies varied considerably from month to month. Just using the individual March and July values probably did not provide an appropriate sample.

The comparison of transition dates to predicted mixed layer temperature behavior proved to be a more successful relationship. The latitude and longitude displays of model-predicted temperature traces from March to July were used. The differences between each trace were graphically displayed as in Fig. 20, with positive areas defined when the 1976 temperature trace was greater than the 1977 trace. The actual mixed layer temperatures would not have had the same representation between the years, because the initial values for

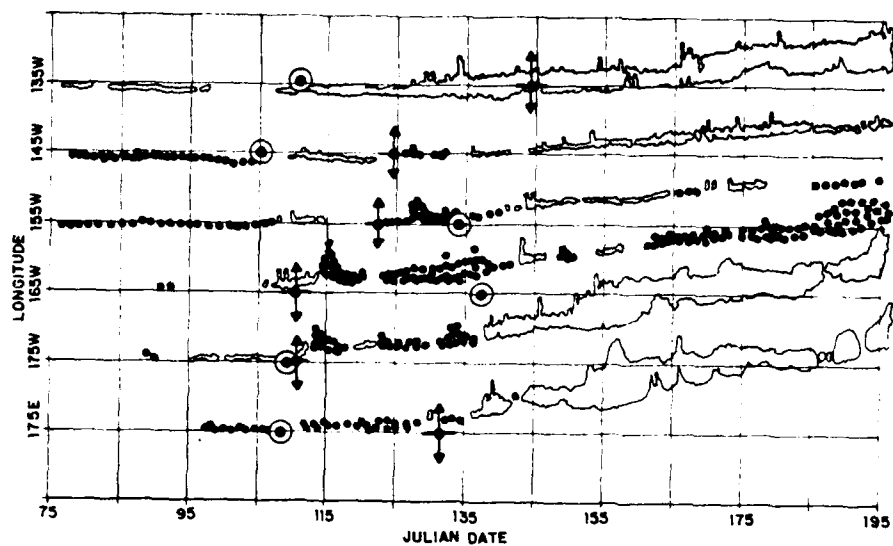


Fig. 20 Difference in mixed layer temperature (1976 minus 1977) at points along 38°N with positive values enclosed in envelope and negative values in dotted regions. Transition dates: 1976 (circle), 1977 (cross). Each 10° longitude corresponds to 3.1C.

both years were not equal. All of the 1977 initial temperatures were 1 to 2 C lower than those in 1976, except that values of less than 1 C higher were found along 135°W. This comparison did not portray the differences in actual temperatures, but rather, the behavior of the relative temperatures with respect to the transition date.

The relative seasonal heating was defined as the net difference in mixed layer temperature from the earlier of the two transition dates at each location to July 15. A difference in net heating in degree days was graphically estimated from the positive and negative areas of each of the coupled traces. If the transition date came earlier in 1976 than in 1977, then there should have been greater heat gain at that location in 1976. The two or three month estimate of mixed layer heat changes was sufficient time over which to determine the existence of the transition-temperature relationship.

The behavior of the difference of relative mixed layer temperature (1976 minus 1977) at points along 38°N is exhibited in Fig. 20. Each 10° of longitude on the figure corresponds to 3.1 C. The uppermost record (135°W) showed a steadily increasing positive difference, beginning with the 1976 transition date. At 175°E, a large net positive difference developed at a much later time. The temperature changes at 175°W and 155°W did not correspond well with the transition date placements. At 165°W, however, the 1977 transition date

was much earlier than in 1976, and a correspondingly large negative accumulation developed.

In general, the behavior of the coupled traces for both years over the ADS area revealed that considerably more relative seasonal heating was realized in the southwestern portion than in other parts. At  $32^{\circ}\text{N}$ ,  $175^{\circ}\text{E}$  a temperature rise of nearly 9 C was predicted for the 4-month period, whereas at  $32^{\circ}\text{N}$ ,  $135^{\circ}\text{W}$  only a 1.5 to 3 C rise was predicted. Along  $175^{\circ}\text{W}$ , predicted temperature increases through the time series were from 4 to 6 C in the south, and from 2 to 3 C in the north. Along  $155^{\circ}\text{W}$ , the temperature increases (2 to 4 C) were similar at all latitudes. These smaller increases were attributable to the later transition dates along this longitude.

The difference between the transition dates versus the net accumulated heat (degree days) from the earlier transition date to Julian day 195 for all locations was plotted in Fig. 21. It was expected that a linear relationship of an increasingly negative difference in transition dates corresponded to an increasingly large value of accumulated heating. A majority of points followed this pattern closely. More points appeared in the upper left quadrant because a greater number of transition dates were earlier in 1976. The points that do not follow the linear relationship may have been the result of a false transition date, or errors

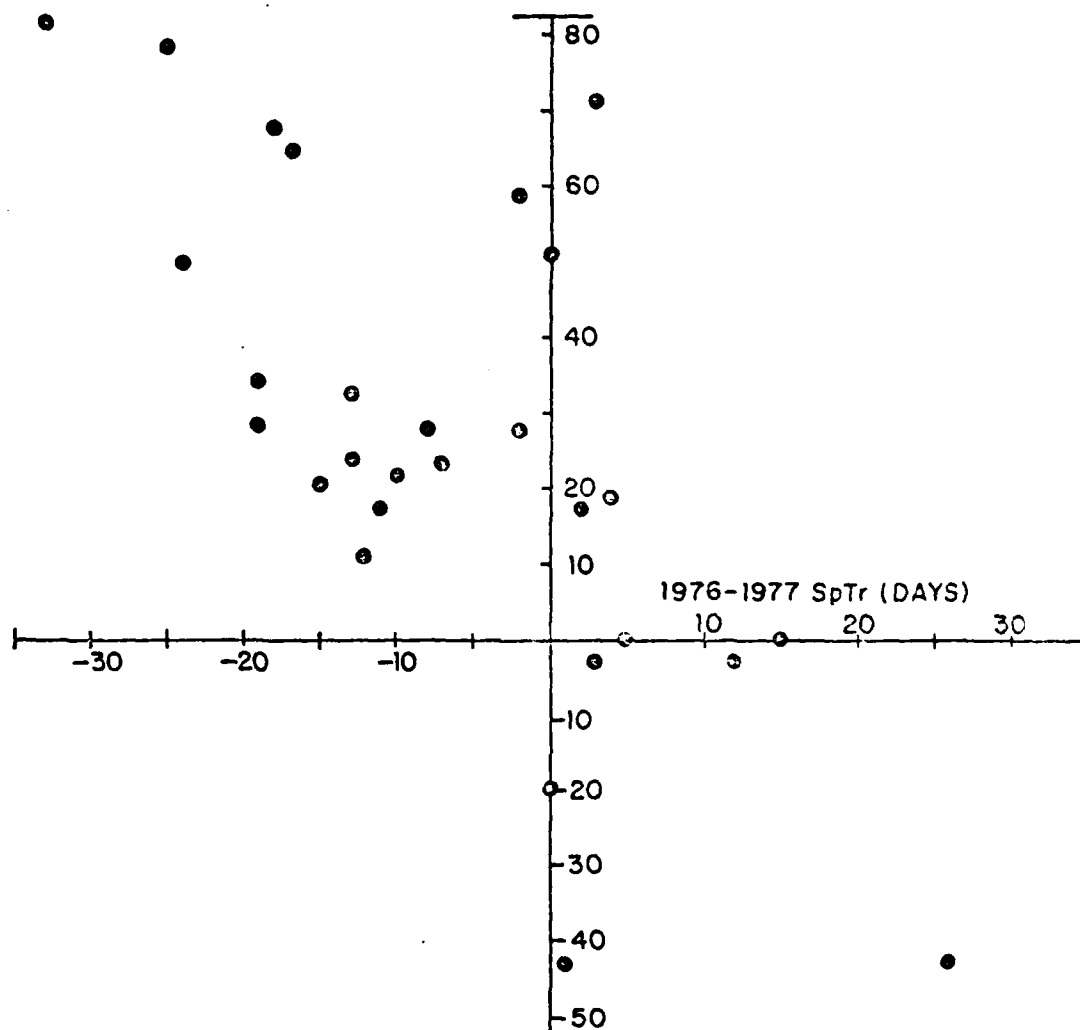


Fig. 21 Difference between the transition date versus the net accumulated temperature increase ( $^{\circ}\text{C}$  days) from the earlier transition date (1976 or 1977) to day 195 for all locations shown in Fig. 1.



in the estimate of accumualted heat. The concept of an earli-  
er transition date leading to a higher sea-surface temperature,  
appears to have been verified for this sample.

## X. CONCLUSIONS

The ocean thermal structure changes for the spring of 1976 and 1977 were predicted with reasonable accuracy. Better observational resolution of the forcing parameters, provided by FNOC, and more detailed ocean thermal analyses, would likely improve the prediction/verification capability. The mixed layer temperature change has been shown to be related to one-dimensional processes to first order. Non-local effects were significant in some regions, so a parameterization of these effects, would be desirable in any attempt to improve prediction capability.

The atmospheric forcing package from FNOC was acceptable, except the total heat flux calculations had to be altered by a correction field before being used by the mixed layer model. Even though synoptic and diurnal wind oscillations were the primary influence on ocean thermal structure changes, accurate specification of the solar and total heat flux were also required.

The ocean thermal behavior within the ADS area for each spring period was similar. In 1976 and 1977, the southeastern portion had the largest heat content in March. By June the heat content distribution was zonally uniform throughout the southern part. Diurnal influences on wind and mixed layer depth were greater in the southern part. Data at

additional locations within the ADS area should be evaluated for better spatial resolution of the transition dates. Data from other years should be compiled, so that normal transition dates can be estimated. Use of the method of executing the model at ADS grid points simultaneously, instead of individually, would facilitate the additional computations.

The objective method for selecting a spring transition date was effective, even though it had limitations at far northern latitudes of the ADS area. Correct dates were crucial in the determination of a transition-temperature anomaly relationship. The spring transition usually occurred within a 36-hour period; however, the time period for transition was longer for steady wind conditions. Atmospheric high pressure areas were usually found over locations undergoing transition. The mixed layer depths and wind speed were statistically different before and after the transition dates. The evaluation and verification procedures used in the study led to an indeterminant judgement as to whether the one-dimensional mixed layer model accurately predicted the observed sea-surface temperature anomalies. However, the model results did lead to the confirmation that earlier transition dates were associated with higher predicted sea-surface temperatures.

## APPENDIX

### SYSTEM PROGRAMS

A sequence of programs was used to achieve the desired output of the predicted oceanic time series. These programs were developed and tested by Patrick Gallacher, in research supported by the Naval Ocean Research and Development Activity. The forcing fields were retrieved from an edited data tape for the period March 15 through July 15 in 1976 and 1977. The RTRVID program read a control card and translated the given latitude and longitude point into array indicies. The beginning date-time was changed into a Julian date, and an ending date-time, was computed using the requested number of days for retrieval. The input file was searched, and all records with requested catalog numbers which fell between the starting and stopping time were extracted and placed in the output files by catalog number. Then, program CRCTID replaced any missing fields by values derived by linear interpolation of the adjacent values in time.

An instantaneous solar flux estimate which was available from the FNOG atmospheric prediction model each 12 hours, normally provided only one daytime value. Program AllILD interpolated the values of solar radiation to 1-hour intervals during the remainder of the daylight hours. Milankovich's formula [Gallacher, 1979] was used to estimate the hourly

solar flux, utilizing the value of the solar flux closest to local noon and time of local sunrise and sunset. This procedure assumed that the moisture and cloudiness effects that were implied in the known solar flux value persisted throughout the daylight hours. The interpolated values were then written on a file, and the values for nighttime hours were set to zero.

The 12-hour total heat fluxes were determined by subtracting the original solar flux from the total heat values. The residual heat flux was interpolated to 1-hour intervals, using the International Mathematics and Statistics Library (IMSL, 1979) cubic spline routines. The values of solar radiation at 1-hour intervals were then added (program A18I1D) to the interpolated residual heat flux to obtain the total heat flux at 1-hour intervals.

The E-W and N-S wind components at 6-hour intervals were interpolated using cubic splines to 1-hour intervals by program FRCF1D. The results were written on a new file, which was then used by program WNDS1D to form a wind speed from the component values, by using the Pythagorean relationship.

Garwood's bulk mixed layer model was initialized with TRANSPAC temperature profile for a given location and month (March). Program OBLM1D performed this task by: locating the simulated bathythermograph (BT) profile corresponding to the requested starting time and grid point, then linearly

interpolating the profile to 1-meter depths. As each day of forcing was read, the model ran forward for that day, deepening or shallowing the mixed layer in response to the atmospheric forcing. The output files of the mixed layer depth/temperature and temperature profiles were generated in 3-hour increments, as specified in the program. The processing continued in this manner, until the entire 122-day time series of forcing had been used.

## BIBLIOGRAPHY

- Camp, N. T., and R. L. Elsberry, 1978: Oceanic Thermal response to Strong Atmospheric Forcing. II. Simulations with Mixed Layer Models. J. Phys. Oceanogr., 8, 215-224.
- Elsberry, R. L., and N. T. Camp, 1978: Oceanic Thermal Response to Strong Atmospheric Forcing. I. Characteristics of Forcing Events. J. Phys. Oceanogr., 8, 206-214.
- Elsberry, R. L., P. C. Gallacher, R. W. Garwood, Jr., 1979: One-dimensional Model Predictions of Temperature Anomalies During Fall 1976. Naval Postgraduate School Technical Report NPS 63-79-003, 30 pp.
- Elsberry, R. L., and R. W. Garwood, Jr., 1978: Sea-surface Temperature Anomaly Generation in Relation to Atmospheric Storms. Bull. Am. Meteor. Soc., 59, 786-789.
- Elsberry, R. L., and R. W. Garwood, Jr., 1979: First-generation Numerical Ocean Prediction Models--Goal for the 1980's. Naval Postgraduate School Technical Report NPS 63-79-007, 41 pp.
- Elsberry, R. L. and S. D. Raney, 1978: Sea-surface Temperature Response to Variations in Atmospheric Wind Forcing. J. Phys. Oceanogr., 8, 881-887.
- Gallacher, P. C. 1979: Preparation of Ocean Modeling Parameters from FNWC Atmospheric Analyses and Model Predictions. Naval Postgraduate School Technical Report NPS 63-79-005, 24 pp.
- Garwood, R. W. Jr., 1977: An Oceanic Mixed Layer Model Capable of Simulating Cyclic States. J. Physic Oceanogr., 7, 455-468.
- Naval Marine Fisheries Service, 1976, 1977: Sea Surface Temperature and Environmental Conditions. Fishing Information, Southwest Fisheries Center-La Jolla, CA, 3,4,5,6,7.
- Roscoe, J. T., 1969: Fundamental Research Statistics for the Behavioral Sciences, Holt, Rinehart, and Winston, pp. 137-139, 156-169.
- Snedecar, G. W., and W. G. Cochran, 1967: Statistical Methods, 6th Ed., Iowa State Univ. Press, pp. 100-106.

White, W. B., and R. L. Bernstein, 1979: Design of an  
Oceanographic Network in the Midlatitude North Pacific.  
J. Phys. Oceanogr., 9, 592-606.



# INITIAL DISTRIBUTION LIST

	No. copies
1. ATTN: WFE6x2 (Personnel) National Weather Service Eastern Region 585 Stewart Ave. Garden City, NY 11530	1
2. Chief, Scientific Services Division (WFE3) National Weather Service Eastern Region 585 Stewart Ave. Garden City, NY 11530	1
3. National Weather Service Forecast Office P. O. Box 3563 Portland, ME 04104	1
4. Bruce W. Budd 4 City View Rd. Cape Elizabeth, ME 04107	2
5. Art Pore Techniques Development Lab, NWS/NOAA Silver Spring, MD 20907	1
6. Library, Code 0142 Naval Postgraduate School Monterey, California 93940	2
7. Defense Technical Information Center Cameron Station Alexandria, Virginia 22314	2
8. Dr. J. T. Haltiner, Code 63Ha Chairman, Department of Meteorology Naval Postgraduate School Monterey, CA 93940	1
9. Dr. R. L. Elsberry, Code 63Es Department of Meteorology Naval Postgraduate School Monterey, CA 93940	6
10. Dr. R. W. Garwood, Jr., Code 68Gd Department of Oceanography Naval Postgraduate School Monterey, CA 93940	1

11. Mr. P. C. Gallacher, Code 63 1  
Department of Meteorology  
Naval Postgraduate School  
Monterey, CA 93940
12. Commanding Officer (Attn: S. Piacsek) 1  
Naval Ocean Research and Development Agency  
NTSL Station, MS 39529
13. Commanding Officer 1  
Fleet Numerical Oceanography Center  
Monterey, CA 93940
14. Commander 1  
Naval Oceanography Command  
NTSL Station, MS 39529
15. Dr. Robert L. Haney, Code 63Hy 1  
Department of Meteorology  
Naval Postgraduate School  
Monterey, CA 93940
16. Dr. Warren White 1  
Scripps Institution of Oceanography A-030  
La Jolla, CA 92093
17. Commander 1  
Oceanographic Systems Pacific  
Box 1390  
Pearl Harbor, HI 96860